

# NAVAL POSTGRADUATE SCHOOL Monterey, California

2

AD-A277 041



DTIC  
ELECTE  
MAR 23 1994

F

D



## THESIS

94-09092



PULSE-SPLITTING AND AM-FM CONVERSION IN A  
NONLINEAR DISPERSIVE MEDIUM

by

William F. Coleman

December, 1993

Thesis Advisor:  
Co-advisor:

Andrés Larraza  
Anthony A. Atchley

Approved for public release; distribution is unlimited.

94 3 22 012

REPORT DOCUMENTATION PAGE			Form Approved OMB No. 0704
Public reporting burden for this collection of information is estimated to average 1 hour per response, including the time for reviewing instruction, searching existing data sources, gathering and maintaining the data needed, and completing and reviewing the collection of information. Send comments regarding this burden estimate or any other aspect of this collection of information, including suggestions for reducing this burden, to Washington Headquarters Services, Directorate for Information Operations and Reports, 1215 Jefferson Davis Highway, Suite 1204, Arlington, VA 22202-4302, and to the Office of Management and Budget, Paperwork Reduction Project (0704-0188) Washington DC 20503.			
1. AGENCY USE ONLY (Leave blank)	2. REPORT DATE 01Dec1993.	3. REPORT TYPE AND DATES COVERED Master's Thesis	
4. TITLE AND SUBTITLE Pulse Splitting And AM-FM Conversion in a Nonlinear Dispersive Medium		5. FUNDING NUMBERS	
6. AUTHOR(S) William F. Coleman		8. PERFORMING ORGANIZATION REPORT NUMBER	
7. PERFORMING ORGANIZATION NAME(S) AND ADDRESS(ES) Naval Postgraduate School Monterey CA 93943-5000		10. SPONSORING/MONITORING AGENCY REPORT NUMBER	
9. SPONSORING/MONITORING AGENCY NAME(S) AND ADDRESS(ES)		10. SPONSORING/MONITORING AGENCY REPORT NUMBER	
11. SUPPLEMENTARY NOTES The views expressed in this thesis are those of the author and do not reflect the official policy or position of the Department of Defense or the U.S. Government.			
12a. DISTRIBUTION/AVAILABILITY STATEMENT Approved for public release; distribution is unlimited.		12b. DISTRIBUTION CODE A	
13. ABSTRACT (maximum 200 words) Experimental and theoretical results are presented for nonlinear dispersive waveguide modes in an acoustic duct. We report observations of a localized envelope which splits into two disturbances moving with two different velocities of propagation. As a consequence, we predict that if a signal is amplitude modulated at the source, spatial beating between the two disturbances will occur, and at periodic positions in space the signal will become frequency modulated. These results can have applications in an all-optical AM-FM conversion and in high data rate fiber optic communications.			
14. SUBJECT TERMS Acoustics; Nonlinear Acoustics		15. NUMBER OF PAGES 74	
		16. PRICE CODE	
17. SECURITY CLASSIFICATION OF REPORT Unclassified	18. SECURITY CLASSIFICATION OF THIS PAGE Unclassified	19. SECURITY CLASSIFICATION OF ABSTRACT Unclassified	20. LIMITATION OF ABSTRACT UL

NSN 7540-01-280-5500

Standard Form 298 (Rev. 2-89)

Prescribed by ANSI Std. Z39-18

Accession For	
NTIS	CRA&I
DTIC	TAB
Unannounced	
Justification	
By	
Distribution/	
Availability Codes	
Dist	Avail and/or Special
A-1	

Approved for public release; distribution is unlimited.

Pulse-Splitting and AM-FM Conversion  
in a Nonlinear Dispersive Medium

by

William F. Coleman  
Lieutenant, United States Navy  
B.S., Southeastern Louisiana University, 1983

Submitted in partial fulfillment  
of the requirements for the degree of

MASTER OF SCIENCE IN PHYSICS

from the

NAVAL POSTGRADUATE SCHOOL  
December 1993

Author:

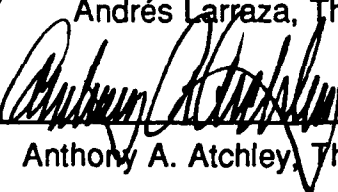


William F. Coleman

Approved by:



Andrés Larraza, Thesis Advisor



Anthony A. Atchley, Thesis Co-advisor



William B. Colson, Chairman  
Department of Physics

## **Abstract**

Experimental and theoretical results are presented for nonlinear dispersive waveguide modes in an acoustic duct. We report observations of a localized envelope which splits into two disturbances moving with two different velocities of propagation. As a consequence, we predict that if a signal is amplitude modulated at the source, spatial beating between the two disturbances will occur, and at periodic positions in space the signal will become frequency modulated. These results can have applications in an all-optical AM-FM conversion and in high data rate fiber optic communications.

## TABLE OF CONTENTS

1. INTRODUCTION .....	1
2. ONE DIMENSIONAL MODULATION THEORY .....	13
1. LINEAR MODULATION THEORY IN ONE DIMENSION .....	13
a. Kinematic Considerations .....	13
b. Energy Propagation .....	15
2. NONLINEAR WAVES .....	17
3. GROUP VELOCITY SPLITTING .....	19
1. PULSE SPLITTING .....	19
2. THE EIGENVALUE PROBLEM .....	21
3. AMPLITUDE MODULATION TO FREQUENCY MODULATION ...	24
4. SOUNDWAVES IN A CYLINDRICAL WAVEGUIDE .....	27
1. LINEAR THEORY .....	27
2. THE NONLINEAR COEFFICIENT .....	32
5. EXPERIMENTAL RESULTS .....	43
1. EXPERIMENTAL APPARATUS .....	43
2. EXPERIMENTAL RESULTS .....	46
a. Frequency Response .....	46

b. Attenuation Constant .....	49
c. Group Velocity Measurements .....	51
d. Measurements of Pulse Spreading .....	53
e. Measurement of the Nonlinear Coefficient .....	55
f. Measurement of Group Velocity Splitting .....	58
 6. CONCLUSIONS, POTENTIAL APPLICATIONS, AND FUTURE WORK .....	 63
1. CONCLUSIONS .....	63
2. POTENTIAL APPLICATIONS .....	64
3. FUTURE WORK .....	65
 REFERENCES .....	 66
 INITIAL DISTRIBUTION LIST .....	 67

## CHAPTER 1. INTRODUCTION

Nonlinearity can give rise to behavior that is fundamentally different from linear behavior. Solitons are the most dramatic example where an exponentially localized wave of constant shape is the result of a stable balance between nonlinearity, which causes the wave to shock, and dispersion, which causes the wave to spread. Among the most well known examples of solitons are the envelope solitons. These solitons are the result of an instability whereby an amplitude modulation superimposed on a wavetrain initially grows and eventually self-localizes. As we will see below, this instability is realized if the product of the nonlinear coefficient and the curvature of the dispersion curve (frequency vs. wavenumber) is negative.

When the product of the nonlinear coefficient and the curvature of the dispersion curve is positive, modulations of a nonlinear wave are stable. In this case, the most striking feature resulting from the nonlinear action is that a modulation of finite extent will split into two disturbances moving with two different velocities of propagation (Whitham, 1974). This behavior should be contrasted with linear theory where such a disturbance will undergo distortion due to dispersion, but will not split. To our knowledge, no experimental evidence of this effect has been pursued to the present, with the exception of this work.

We can gain a physical understanding of amplitude modulations of nonlinear dispersive waves by considering independently the effects of dispersion and

nonlinearity on a wave. Although the ideas below are very general, we will develop the conceptual background for acoustics in a waveguide, as this is the system that we use for our experiment.

A harmonic plane wave propagating in free space or in a waveguide below cutoff satisfies the dispersion relation  $\omega = ck$ , where  $\omega$  is the frequency of the wave,  $k$  is the wavenumber of the wave, and  $c$  is the speed of sound in the medium. That is the frequency is proportional to the wavenumber and the phase velocity equals the slope  $d\omega/dk$  of the line in the  $\omega$ - $k$  plane. In this case, the phase and group velocities are independent of frequency. Therefore, a group or superposition of harmonic waves with different frequencies all travel together with the same speed.

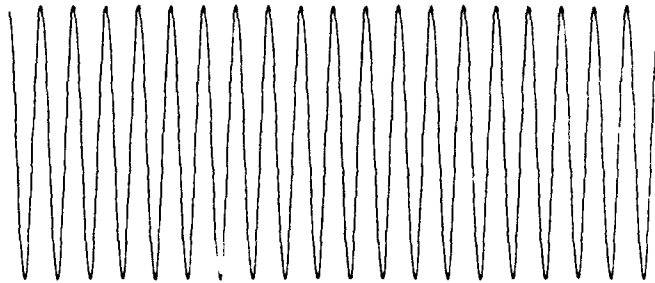
However, for acoustic propagation in a waveguide above cutoff the dispersion relation has curvature (i.e.,  $d^2\omega/dk^2 \equiv \omega''(k) \neq 0$ ). Hence the phase velocity is frequency dependent and a group of waves of different frequency - and therefore speeds - will change shape as it propagates. Since the motion of the wave group can no longer be described by a single velocity, a group velocity  $v_g = d\omega/dk$  is defined. The group velocity gives the velocity of propagation of a group of waves extending over a frequency range small compared to the center frequency of the group.

To clarify the concepts of the phase and group velocities, consider an observer in a frame moving with the phase velocity. In this frame an unmodulated wave is described by a stationary pattern of crests and troughs fixed in space and the different points on the wave correspond simply to points of different phase (Fig. 1.1a). To an observer in this frame, a modulated wave



would also appear as a pattern of crests and troughs fixed in space (Fig. 1.1b). However if  $\omega''(k) \neq 0$ , energy flows from regions of high to low amplitude with the group velocity and the amplitude of the crests and troughs would vary in time. Thus an observer fixed in a frame moving with the phase velocity would observe a propagating modulation with a relative speed  $|v_p - v_g|$ .

a )



b )

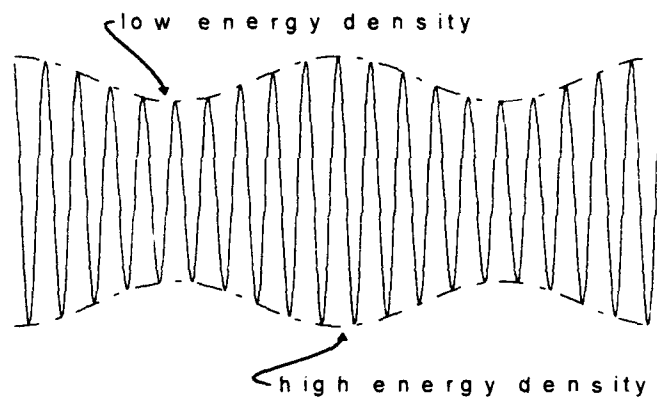
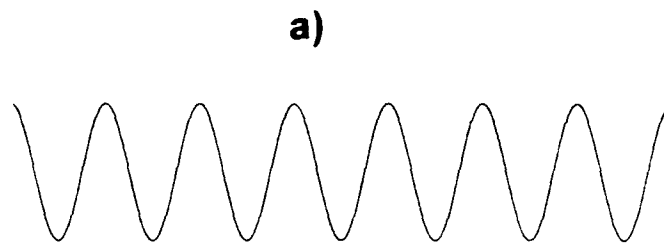


**Fig. 1.1** a) Unmodulated and b) modulated wave in a frame moving with the phase velocity  $v_p$ .

For large amplitude acoustic waves nonlinear effects become important. For plane waves in a nondispersive medium, distortion of the sound wave results from amplitude dependent effects. Since the wave speed is proportional to the square root of the temperature, it follows that compressions, where the temperature is higher, propagate faster than rarefactions, where the temperature is lower. Also, at the compression the particle velocity is in the direction of propagation and at a rarefaction the particle velocity is in the opposite direction. Shock formation of the waveform results in the sawtooth shape shown in Fig. 1.2a as the crests of the wave overtake the troughs.

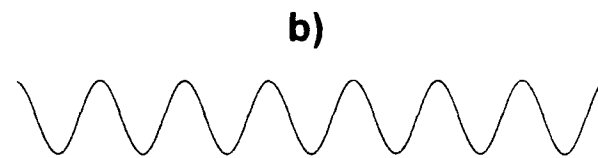
For a dispersive medium shocks are not produced because frequency and wavenumber are not proportional and thus new propagating modes are not generated by nonlinear interactions. However, due to self interaction effects, the frequency of the wave is amplitude dependent and in the weakly nonlinear regime it is of the form  $\omega = \omega_0(k) + \omega_2(k)p^2$ . In this expression,  $\omega_0(k)$  is the linear dispersion relation,  $\omega_2(k)$  is the nonlinear coefficient, and  $p$  is acoustic pressure. For the case of fixed frequency and  $\omega_2 > 0$ , the effect of nonlinearity is to decrease the wavenumber  $k$  as the amplitude of the acoustic field increases. Equivalently, for fixed frequency, as the amplitude of the wave is increased the phase velocity increases.

Because the changes in the wavenumber vary linearly with  $p^2$ , the relative phase between two points fixed in space should also vary in this manner. In Chapter 5 we present experimental results that verify this effect for the (1,0) cylindrical waveguide mode. This result is the first experimental observation of the dependence of the relative phase on the wave amplitude.



**before**

**after**



$$\omega = \omega_0(k) + \omega_2(k)p^2$$

$$\omega_2 > 0$$

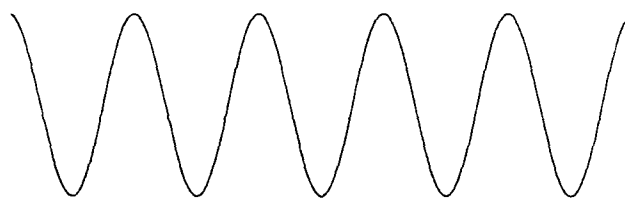


**Fig. 1.2** a) Shock formation resulting from nonlinearity in a nondispersive medium as viewed in a frame moving with the speed of sound. b) For  $\omega_2 > 0$  and fixed frequency, the effect of nonlinearity in dispersive acoustics is to increase the wavelength.

To understand the combined effects of dispersion and nonlinearity, consider an initial state of a modulated wave observed in a frame moving with the group velocity (Fig. 1.3a). Because of dispersion, the group and phase velocities are different and an observer in this frame would see the crests of the wave propagate. If the phase velocity is bigger than the group velocity (as is the case for a mode above cutoff in a waveguide) the crests of the wave will propagate in the positive  $x$  direction.

Without loss of generality we can assume that the nonlinear coefficient  $\omega_2 > 0$ . Thus, the phase velocity in the regions of higher amplitude is greater than in regions of lower amplitude. As a result, an observer in the frame moving with the linear group velocity would observe bunching of the crests at the leading edge of the modulation and anti-bunching at the trailing edge (Fig. 1.3b). For negative dispersion,  $\omega''(k) < 0$ , the long waves travel faster than the short waves and an instability sets in. Dispersive effects cause the energy to approach the crests of the envelope, and the amplitude at the crest increases. This in turn accelerates the instability. Deep gravity waves on the surface of a liquid is an example of a wave system with negative dispersion. For positive dispersion,  $\omega''(k) > 0$ , short waves travel faster than long waves. In this case dispersive effects cause the energy to approach the troughs of the envelope and the modulation propagates. In other words, to an observer moving with the linear group velocity, the modulation is no longer stationary. Acoustic propagation in a waveguide above the cutoff frequency is an example of a wave system with positive dispersion.

In general, if the product  $\omega_2 \omega''$  is negative a modulation will initially grow and the instability will eventually lead to the formation of envelope solitons. If the

product  $\omega_2 \omega''$  is positive, the modulations are stable. In Chapter 4 we calculate the nonlinear coefficient for the (1,0) mode in a cylindrical waveguide and show that it changes sign from positive to negative as the frequency is increased. For this mode, finite extent modulations of a uniform wavetrain are stable below a frequency approximately twice the cutoff frequency and are unstable beyond this frequency .

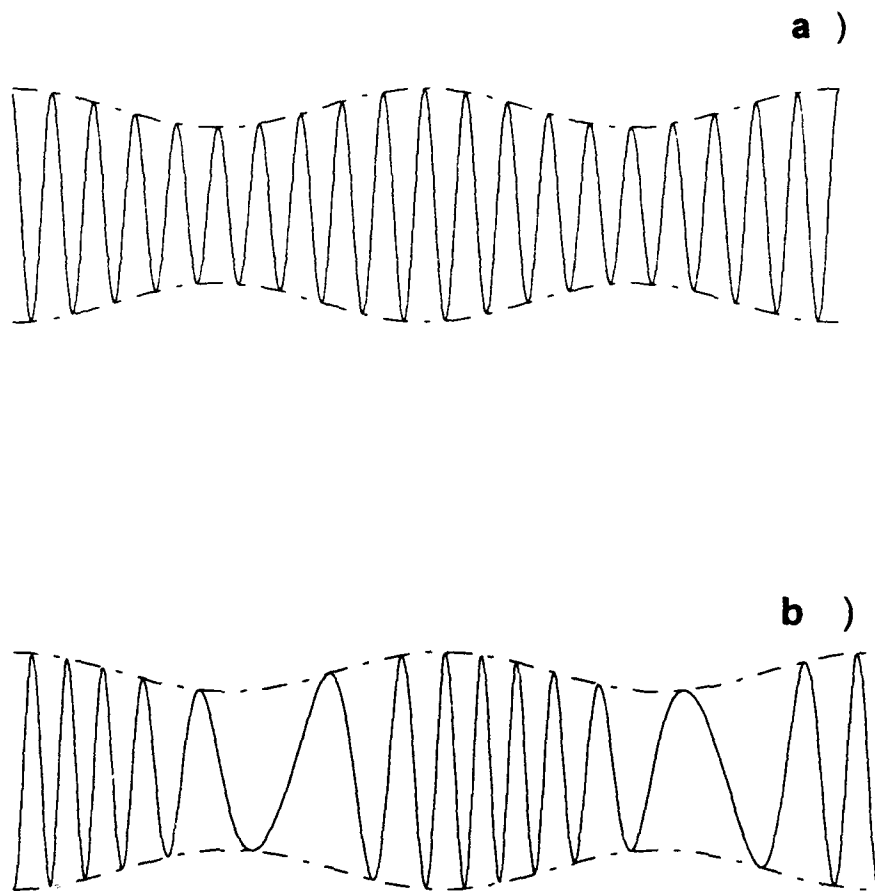


**Fig. 1.3** a) Initial state of a modulated wave in the frame moving with the group velocity  $v_g$ . b) For  $\omega_2 > 0$ , in a frame moving with  $v_g$  nonlinearity results in bunching of the crests at the leading edge of the modulation and anti-bunching of crests at the trailing edge.

The stability of the modulation has two important consequences. One is AM-FM conversion. The other is pulse splitting. Both effects can be physically understood by considering again a modulated wave in a frame moving with the linear group velocity. In this frame, an observer at a fixed location would see alternating bunching and anti-bunching of the wave crests (Fig. 1.4). Because dispersive effects cause the energy to approach the troughs of the envelope, for this observer it would appear that at some time a frequency modulation is imposed upon the amplitude modulated signal. The combined dispersion and nonlinearity cause the energy flow from the short wavelength to the long wavelength of the FM modulation and an amplitude modulation  $180^\circ$  out of phase with respect to the original signal results at a later time. In the frame moving with the group velocity, the process repeats periodically and an observer in this frame sees that the modulations experience beats. In the laboratory frame if a source is generating an amplitude modulated signal, some distance away it will become frequency modulated. This spatial beating of the modulation can be only be understood if for each modulation frequency there correspond two group velocities of propagation.

The splitting of a single high intensity modulated wave has been verified experimentally and is reported in Chapter 5. A single pulse modulation on a CW is observed to split into two pulses. The time difference between them increases both with distance and amplitude.



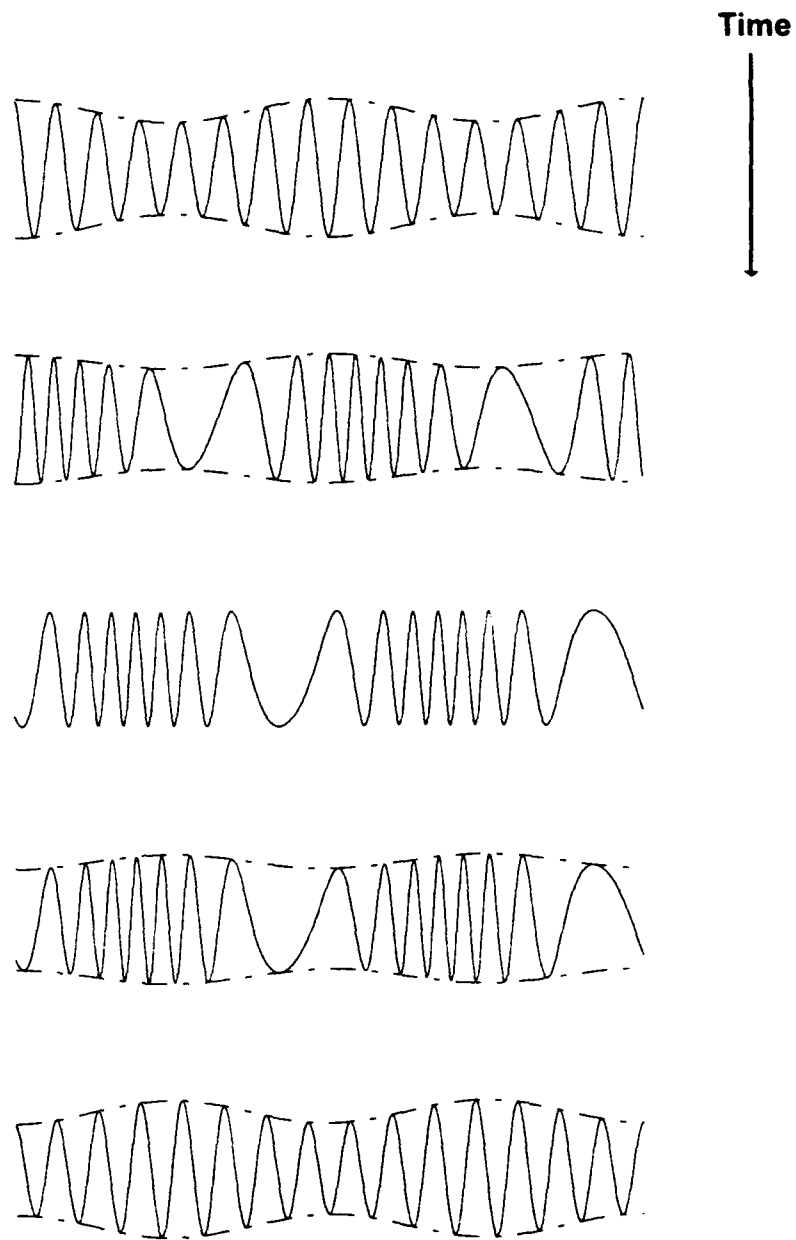


**Fig. 1.4** An observer in a frame moving with the linear group velocity observes AM to FM conversion in time.

The organization of this work is as follows. In Chapter 2 we derive the coupled wavenumber and energy conservation equations. Chapter 3 deals with the quantitative derivation of group velocity splitting. As a consequence of group velocity splitting we predict the existence of AM-FM conversion in modulationally stable nonlinear dispersive systems. In Chapter 4 we apply these results to the specific case of the (1,0) mode in a waveguide of circular cross section. A calculation of the nonlinear coefficient  $\omega_2$  for this mode is presented and the experimental consequences of these results are analyzed. In Chapter 5 we present the experimental results for a nonlinear (1,0) mode in an acoustic duct for the frequency regime that leads to modulational stability. Finally, Chapter 6 summarizes the results of our theoretical and experimental investigations of this phenomena.

## CHAPTER 2. ONE DIMENSIONAL MODULATION THEORY

In this chapter we review the theory of one dimensional modulation of linear waves in a dispersive medium. We then expand our discussion to include the effects of nonlinearity and the combined effects of both nonlinearity and dispersion. Our treatment parallels the work done by Whitham (1974).

### 1. LINEAR MODULATION THEORY IN ONE DIMENSION

#### a) Kinematic Considerations

If the amplitude and propagation wavenumber of a traveling wave vary only slightly over distances of the order of one wavelength, the wave can be described locally by assuming a slowly varying amplitude and phase. A wave field  $\Psi$  can then be described by the expression

$$\Psi = a(x,t)e^{i\theta(x,t)} , \quad (2.1.1)$$

where  $a(x,t)$  is the local value of the amplitude. Over small regions of space and short intervals of time the phase  $\theta(x,t)$  can be expanded in a Taylor series and up to first order, we obtain

$$\theta = \theta_0 + x \frac{\partial \theta}{\partial x} + t \frac{\partial \theta}{\partial t} , \quad (2.1.2)$$

where  $\theta_0$  is the phase evaluated at the origin at time  $t=0$ .

Over small regions of space and during short time intervals, we define the local wave number and frequency at each point as

$$k(x, t) = \frac{\partial \theta}{\partial x} \quad , \quad \omega(x, t) = -\frac{\partial \theta}{\partial t} \quad (2.1.3)$$

Thus, points of constant phase move with velocity

$$c_p = \frac{dx}{dt} = \frac{\omega}{k} \quad (2.1.4)$$

An observer following a particular crest moves with the local phase velocity but in general sees the local wave number and frequency changing; that is neighboring crests get farther away.

By eliminating the phase  $\theta$  from each expression in Eq. (2.1.3), we obtain

$$\frac{\partial k}{\partial t} + \frac{\partial \omega}{\partial t} = 0 \quad (2.1.5)$$

Equation (2.1.5) has the form of a conservation law, where the wavenumber  $k$  in the first term corresponds to the density of waves or number of wave crests per unit length and the frequency  $\omega$  in the second term corresponds to the wave flux or number of wave crests crossing the position  $x$  per unit time.

Equations (2.1.1) - (2.1.3) can be extended to include the case of two and three dimensions. However, the one dimensional equations are sufficient to describe waveguide propagation and we will use them exclusively throughout our discussion.

### b) Energy Propagation

For a general dispersion relation  $\omega = \omega(k)$  the phase velocity is in general frequency dependent. Thus, if a disturbance consists of a group of individual harmonic waves of different frequencies and hence speeds, the resulting wave shape will change with position and the motion of the wave group cannot be described in terms of a single wave velocity.

The general form for a propagating wave in a linear dispersive medium with dispersion relation  $\omega(k)$  is

$$\Psi(x, t) = \int F(k) e^{ikx - i\omega(k)t} dk \quad (2.1.6)$$

For a modulated wavetrain with most of the energy in wavenumbers close to some value  $k_0$ ,  $F(k)$  is concentrated near  $k=k_0$  and (2.1.6) may be approximated by

$$\Psi(x, t) = \int F(k) \exp\{[ikx - i\{\omega(k_0) + (k - k_0)\omega'(k_0)\}t]\} dk \quad (2.1.7)$$

This in turn may be written as  $\Psi = a(x - \omega'(k_0)t) \exp\{i(k_0x - \omega(k_0)t)\}$  where

$$a(x - \omega'(k_0)t) = \int F(k_0 + \kappa) \exp[i\kappa(x - \omega'(k_0)t)] d\kappa \quad (2.1.8)$$

and where we have substituted  $k = k_0 + \kappa$ . The function  $a(x - \omega'(k_0)t)$  describes the modulations of the wave field about  $k_0$ . It varies with  $x$  and  $t$  in such a way that it remains constant when viewed from a coordinate system moving with the *group velocity*

$$c_g = \frac{d\omega}{dk} \quad (2.1.9)$$

evaluated at the center frequency of the group, i. e. at  $\omega = \omega(k_0)$ . Thus, we say that the modulation is constant along the group line  $x = \omega'(k_0) t$ . An observer moving at the group velocity  $\omega'(k_0)$  always sees waves with wavenumber  $k_0$  and frequency  $\omega(k_0)$  but crests keep passing him.

The energy density of a wave is proportional to the square of the wave amplitude. Hence if  $a(x - \omega'(k_0)t)$  is constant in a coordinate system moving with the group velocity, the energy between any two group lines remains constant. In other words,

$$\frac{\partial e}{\partial t} + \frac{\partial}{\partial x}(c_g e) = 0 \quad , \quad (2.1.10)$$

where  $e$  is the energy density. In order to see that (2.1.10) is valid, consider the quantity

$$E(t) = \int_{x_1}^{x_2} a^2 dx = 2\pi \int_{k_1}^{k_2} F(k)F(k)^* dk \quad , \quad (2.1.11)$$

where  $k_1$  and  $k_2$  are defined by

$$x_1 = \omega'(k_1)t \quad , \quad x_2 = \omega'(k_2)t \quad . \quad (2.1.12)$$

If  $k_1$  and  $k_2$  are held fixed as  $t$  varies,  $E(t)$  remains constant. According to (2.1.12), the points  $x_1$  and  $x_2$  are moving with the corresponding group velocities. Thus the total amount of  $a^2$  between any pair of group lines remains the same. Thus  $a^2$  propagates with the group velocity. On the other hand,  $e = f(k) a^2$ , thus (2.1.10) holds provided

$$f(k) \left\{ \frac{\partial a^2}{\partial t} + \frac{\partial}{\partial x} (c_g a^2) \right\} + f'(k) a^2 \left\{ \frac{\partial k}{\partial t} + c_g \frac{\partial k}{\partial x} \right\} = 0. \quad (2.1.13)$$

The first bracket vanishes because  $E(t)$  is constant between any pair of group lines. The second bracket vanishes in view of (2.1.5), the conservation of the number of waves crests!

## 2. NONLINEAR WAVES

The modulations of a linear wavetrain propagating in one dimension in a uniform medium can be described by Eqs. (2.1.5) & (2.1.10). More generally, nonlinearities modify the wave propagation. Nonlinearity results in the appearance of an amplitude dependence in the frequency. For small amplitudes, the frequency dependence on amplitude can be written as

$$\omega(k, a^2) = \omega_0(k) + \omega_2(k) a^2 + \dots, \quad (2.2.1)$$

where  $a$  is the amplitude,  $\omega_0(k)$  is the linear dispersion relation, and  $\omega_2(k)$  is the nonlinear coefficient. Since the energy  $e$  of the wavetrain is proportional to the amplitude squared, Eq. (2.2.1) can also be written

$$\omega(k, e) = \omega_0(k) + \omega_2(k) e + \dots \quad (2.2.2)$$

There are three conditions possible for the nonlinear coefficient  $\omega_2$ . If  $\omega_2(k) = 0$ , the dispersion relation reduces to the linear case. If  $\omega_2(k) < 0$  both

the frequency and phase velocity decrease with increasing amplitude. Finally, if  $\omega_2(k) > 0$ , the frequency and phase velocity increase with increasing amplitude.

An important effect of the nonlinearity is to couple Eqs. (2.1.5) and (2.1.10).

Thus substituting (2.2.2) into (2.1.5) we obtain

$$\frac{\partial k}{\partial t} + (\omega'_0(k) + \omega_2(k)e) \frac{\partial k}{\partial x} + \omega_2(k) \frac{\partial e}{\partial x} = 0 . \quad (2.2.3)$$

For slow modulations of the amplitude, the last term of Eq. (2.2.3) can be as significant as the term  $\omega'_0(k) \partial k / \partial x$ . However, the  $\omega_2(k)e \partial k / \partial x$  term can be ignored for weakly nonlinear fields because it only gives a small correction to the group velocity.

Similarly, in Eq. (2.1.10), we can retain only the linear group velocity and obtain the equations (Whitham, 1974)

$$\frac{\partial k}{\partial t} + \omega'_0(k) \frac{\partial k}{\partial x} + \omega_2(k) \frac{\partial e}{\partial x} = 0 , \quad (2.2.4)$$

$$\frac{\partial e}{\partial t} + \omega'_0(k) \frac{\partial e}{\partial x} + \omega''_0(k)e \frac{\partial k}{\partial x} = 0 . \quad (2.2.5)$$

Equations (2.2.4) and (2.2.5) constitute the basic description for one dimensional nonlinear waves in a uniform dispersive medium. The crucial qualitative change of nonlinearity which couples both equations will be explained in the next chapter.



## CHAPTER 3. GROUP VELOCITY SPLITTING

In this chapter, we consider the general solutions to Eqs. (2.2.4) and (2.2.5). Based on Whitham's modulation theory we will give a quantitative foundation for the splitting of a modulation of finite extent into two separate disturbances. Next, in an extension of these results, we solve the eigenvalue problem for a monochromatic space-time modulation of wavenumber and amplitude. From this we determine that the modulational energy is equipartitioned into two propagating modes. Lastly, we predict that a consequence of nonlinearity on an amplitude modulated signal is to introduce a frequency modulation into the signal and that the reciprocal effect is also possible.

### 1. PULSE SPLITTING

The combined effects of dispersion and nonlinearity on an initial disturbance or a modulation is to couple Eqs. (2.2.4) and (2.2.5)

This system of equations is hyperbolic and in order to determine the characteristic velocity for the system (2.2.4) - (2.2.5), i.e. the velocity on the characteristic along which the wave propagates, we consider the linear combination<sup>&</sup>

---

<sup>&</sup> For an excellent treatment on the classification of partial differential equations and the determination of the family of characteristic curves for hyperbolic equations, the reader must consult Whitham's *Linear and nonlinear waves*.

$$I_1 \left( \frac{\partial k}{\partial t} + \omega'_0(k) \frac{\partial k}{\partial x} + \omega_2(k) \frac{\partial e}{\partial x} \right) + I_2 \left( \frac{\partial e}{\partial t} + \omega'_0(k) \frac{\partial e}{\partial x} + \omega''_0(k) \frac{\partial k}{\partial x} \right) = 0, \quad (3.1.1)$$

which takes the characteristic form

$$I_1 \left( \frac{\partial k}{\partial t} + \frac{dx}{dt} \frac{\partial k}{\partial x} \right) + I_2 \left( \frac{\partial e}{\partial t} + \frac{dx}{dt} \frac{\partial e}{\partial x} \right) = 0, \quad (3.1.2)$$

provided

$$\begin{aligned} I_1 \frac{dx}{dt} &= I_1 \omega'_0(k) + I_2 \omega''_0(k) e, \\ I_2 \frac{dx}{dt} &= I_2 \omega'_0(k) + I_1 \omega_2(k). \end{aligned} \quad (3.1.3)$$

The system of linear algebraic equations (3.1.3) possesses a non-trivial solution when

$$\frac{dx}{dt} = \omega'_0(k) \pm \left( \omega_2(k) \omega''_0(k) e \right)^{1/2}, \quad (3.1.4)$$

and the solutions are real (i.e. propagation is possible) provided  $\omega_2(k) \omega''_0(k) \geq 0$ .

Thus an initial disturbance or a modulation of a source will introduce disturbances into both families of characteristics and consequently two signals moving with different velocities will be detected. This behavior should be contrasted with the linear theory where such a disturbance will undergo distortion due to dispersion, but will not split.

## 2. THE EIGENVALUE PROBLEM

In the previous section we determined that for  $\omega_2(k)\omega_0''(k) \geq 0$ , two real propagating solutions to Eqs. (3.1.3) exist. In this section, we approach the solution of the coupled equations (2.2.4) - (2.2.5) by considering the condition on the values of possible frequencies.

Consider a wavetrain which has been given a space-time modulation of wavenumber and amplitude:

$$k(x,t) = k_0 + \alpha(x,t) , \quad (3.2.1)$$

$$e(x,t) = e_0 + \varepsilon(x,t) , \quad (3.2.2)$$

where  $k_0$  is the unmodulated wavenumber,  $\alpha(x,t)$  is the modulation of the wavenumber,  $e_0$  is the constant energy of the unmodulated carrier, and  $\varepsilon(x,t)$  is the energy of the modulation.

A linearization of Eqs. (2.2.4) and (2.2.5) about the uniform state  $k_0$  and  $e_0$  yields the modulation equations

$$\frac{\partial \alpha}{\partial t} + \omega_0' \frac{\partial \alpha}{\partial x} + \omega_2 \frac{\partial \varepsilon}{\partial x} = 0 , \quad (3.2.3)$$

$$\frac{\partial \varepsilon}{\partial t} + \omega_0' \frac{\partial \varepsilon}{\partial x} + \omega_0'' e_0 \frac{\partial \alpha}{\partial x} = 0 . \quad (3.2.4)$$

If we seek solutions to Eqs. (3.2.3) - (3.2.4) of the form  $\alpha = \alpha_0 e^{i\Omega t - i\kappa x}$  and  $\varepsilon = \varepsilon_0 e^{i\Omega t - i\kappa x}$ , we obtain

$$(\Omega - \omega'_0 \kappa) \alpha_0 - \omega_2 \kappa \epsilon_0 = 0, \quad (3.2.5)$$

$$-\omega''_0 \epsilon_0 \kappa \alpha_0 + (\Omega - \omega'_0 \kappa) \epsilon_0 = 0 \quad (3.2.6)$$

Equations (3.2.5) - (3.2.6) have a non-trivial solution only if

$$\Omega = \omega'_0 \kappa \pm \sqrt{\omega''_0 \omega_2 \epsilon_0} \kappa. \quad (3.2.7)$$

The dispersion relation (3.2.7) shows that for fixed  $\Omega$ , there are two possible wavelengths of the modulated state i.e.

$$q = \frac{\Omega}{(\omega'_0 + \sqrt{\omega''_0 \omega_2 \epsilon_0})}, \quad (3.2.8)$$

$$p = \frac{\Omega}{(\omega'_0 - \sqrt{\omega''_0 \omega_2 \epsilon_0})}. \quad (3.2.9)$$

Because the nonlinearity is weak (i.e.,  $\sqrt{\omega''_0 \omega_2 \epsilon_0} \ll \omega'_0$ ), (3.2.8) and (3.2.9) can be rewritten as

$$q \approx \frac{\Omega}{\omega'_0} \left( 1 - \frac{\sqrt{\omega''_0 \omega_2 \epsilon_0}}{\omega'_0} \right), \quad (3.2.10)$$

$$p \approx \frac{\Omega}{\omega'_0} \left( 1 + \frac{\sqrt{\omega''_0 \omega_2 \epsilon_0}}{\omega'_0} \right). \quad (3.2.11)$$

Because there are two eigenvalues to the set of Eqs. (3.2.3) - (3.2.4), the most general solution for  $\alpha(x, t)$  and  $\varepsilon(x, t)$  for fixed  $\Omega$  must be of the form

$$\alpha(x, t) = u_1 e^{i\Omega t - iqx} + v_1 e^{i\Omega t - ipx}, \quad (3.2.12)$$

$$\varepsilon(x, t) = u_2 e^{i\Omega t - iqx} + v_2 e^{i\Omega t - ipx}. \quad (3.2.13)$$

Substituting solutions (3.2.12) - (3.2.13) into (3.2.3) - (3.2.4) and using the fact that the modes are linearly independent, we obtain

$$(-\Omega + \omega'_0(k)q)u_1 + \omega_2(k)qu_2 = 0 \quad (3.2.14)$$

$$(-\Omega + \omega'_0(k)p)v_1 + \omega_2(k)pv_2 = 0. \quad (3.2.15)$$

Using (3.2.10) and (3.2.11) we obtain

$$\frac{u_1}{u_2} = \sqrt{\frac{\omega_2}{\omega''_0 e_0}}, \quad (3.2.14a)$$

$$\frac{v_1}{v_2} = -\sqrt{\frac{\omega_2}{\omega''_0 e_0}}. \quad (3.2.15a)$$

Equations (3.2.14a) - (3.2.15a) determine the ratios of  $u_1$  to  $u_2$  and  $v_1$  to  $v_2$  respectively. The ratio of  $u_1$  to  $v_1$  and  $u_2$  to  $v_2$  are determined by boundary conditions on the signal.

### 3. AMPLITUDE MODULATION TO FREQUENCY MODULATION

Consider an arbitrary amplitude modulated signal at  $x=0$  of the form

$$a(0, t) = A[1 + m \cos(\Omega t)] \cos(\omega t) , \quad (3.3.1)$$

where  $A$  is the amplitude,  $m$  is the modulation amplitude,  $\Omega$  is the modulation frequency and  $\omega$  is the carrier frequency. At the boundary, Eq. (3.2.13) becomes

$$\varepsilon(0, t) = u_2 e^{i\Omega t} + v_2 e^{i\Omega t} . \quad (3.3.2)$$

Also, at  $x=0$ , the general expression for the phase becomes

$$\theta(0, t) = \frac{i u_1}{q} e^{i\Omega t} + \frac{i v_1}{p} e^{i\Omega t} - \omega t , \quad (3.3.3)$$

where we have integrated the expression,  $\frac{\partial \theta(x, t)}{\partial x} = k_0 + \alpha(x, t)$  for the modulated wavenumber and taken the associated arbitrary function of time in the result to be  $-\omega t$ .

Because at  $x=0$  the amplitude modulated signal is of the form (3.3.1), it follows from Eq. (3.3.3)

$$i \frac{u_1}{q} e^{i\Omega t} + i \frac{v_1}{p} e^{i\Omega t} = 0 . \quad (3.3.4)$$

This requires

$$\frac{u_1}{q} + \frac{v_1}{p} = 0 . \quad (3.3.5)$$

Because the nonlinearity is weak,  $p$  is approximately equal to  $q$  and

$$u_1 \cong -v_1 , \quad (3.3.6)$$

which expresses the fact that energy is equipartitioned between the two propagating modes.

At any point  $x$ , the energy  $\varepsilon(x, t)$  is

$$\varepsilon(x, t) = u_2 [\cos(\Omega t - qx) + \cos(\Omega t - px)] , \quad (3.3.7)$$

where we have considered the real part only. Using trigonometric identities and

defining  $\Delta = \frac{p-q}{2}$  and  $\eta = \frac{p+q}{2}$ , we obtain

$$\varepsilon(x, t) = 2u_2 \cos \Delta x \cos(\Omega t - \eta x) . \quad (3.3.8)$$

If the modulation amplitude  $m$  is small compared to unity, from Eq. (3.3.7)

$$\varepsilon(0, t) = 2A^2 m \cos \Omega t . \quad (3.3.9)$$

Upon comparison with Eq. (3.3.2) we obtain

$$u_2 = A^2 m . \quad (3.3.10)$$

Similarly, at any point  $x$ , the phase  $\theta(x, t)$  is

$$\theta(x, t) = k_0 x - \omega t - \frac{2u_1}{q} \sin(\Delta x) \cos(\Omega t - \eta x) , \quad (3.3.11)$$

and from Eq. (3.2.14a)  $u_1 = \sqrt{\frac{\omega_2}{\omega_0'' e_0}} A^2 m$  .

Also, using the fact that  $q = \Omega / \omega_0'$ , we obtain the following expression for the amplitude modulated wave:

$$a(x, t) = A[1 + 2m \cos(\Delta x) \cos(\Omega t - \eta x)] \\ \times \cos\left[k_0 x - \omega t - \frac{2A^2 m (\omega_0')^2}{\Omega} \sqrt{\frac{\omega_2}{\omega_0'' e_0}} \sin(\Delta x) \cos(\Omega t - \eta x)\right] . \quad (3.3.12)$$

Thus a consequence of the nonlinearity on an amplitude modulated signal is to introduce frequency modulation.

Equation (3.3.12) exhibits reciprocity regarding frequency modulation to amplitude modulation. When  $\cos \Delta x = 0$  the signal is entirely frequency modulated. If we consider this point as the source of the modulated wave, it must follow that a consequence of nonlinearity on an frequency modulated signal is to introduce an amplitude modulation into the signal.



## CHAPTER 4. SOUND WAVES IN A CYLINDRICAL WAVEGUIDE

In this chapter we review the theory of sound wave propagation in a cylindrical waveguide. Following Morse and Ingard (1968), we examine the general linear theory and derive the waveguide dispersion relation. We discuss the perturbation technique of Keller and Millman (1972) that can be used to determine the effect of small finite amplitude of an acoustic wave. We specialize the results of the perturbation method to determine the nonlinear coefficient  $\omega_2$  for the specific case of the first non-axially symmetric mode in a cylindrical waveguide. Lastly, we examine the experimental consequences of our results.

### 1. LINEAR THEORY

The wave equation for simple harmonic waves  $p(x,y,z)e^{i\omega t}$  propagating in an acoustic duct is

$$\left( \frac{\partial^2}{\partial x^2} + \frac{\partial^2}{\partial y^2} + \frac{\partial^2}{\partial z^2} \right) p + \left( \frac{\omega}{c} \right)^2 p = 0 , \quad (4.1.1)$$

where  $p$  is the pressure,  $c$  is the thermodynamic speed of sound in the medium, and  $\omega$  is the angular frequency of the wave. Setting the  $z$  axis parallel to the axis of the duct we seek a solution of the form

$$p = \Psi(x, y)e^{ikz}, \quad (4.1.2)$$

where the factor  $\Psi$  satisfies the equation

$$\left( \frac{\partial^2}{\partial x^2} + \frac{\partial^2}{\partial y^2} \right) \Psi + \gamma^2 \Psi = 0, \quad (4.1.3)$$

with

$$\left( \frac{\omega}{c} \right)^2 = k^2 + \gamma^2, \quad (4.1.4)$$

the waveguide dispersion relation for  $\omega(k)$ .

For a rigid wall duct, the fluid velocity normal to the surface wall must be zero.

From the linearized momentum equation

$$\rho \frac{\partial \hat{u}}{\partial t} = -\nabla p, \quad (4.1.5)$$

a harmonic wave satisfies

$$i\rho\omega\hat{u} = \nabla p \quad (4.1.6)$$

where  $\rho$  is the density and  $u$  is the fluid velocity. Thus, in terms of the acoustic pressure the appropriate boundary condition for a rigid wall is

$$\frac{\partial \Psi}{\partial n} = 0, \quad (4.1.7)$$

for every point on the wall perimeter with  $n$  the normal to the wall.

There exists a discrete set of eigenvalues  $\gamma_j$  for which Eqs. (4.1.3) and (4.1.7) are satisfied. From Eq. (4.1.4) it can be seen that to each mode corresponds a specific cutoff frequency  $c\gamma_j$ . For frequencies  $\omega$  greater than  $c\gamma_j$ ,  $k$  is a real number and the wave propagates along the tube. For frequencies less than  $c\gamma_j$ ,  $k$  is imaginary and the mode does not propagate.

The lowest eigenvalue  $\gamma_0$  corresponds to the fundamental plane wave mode. For this mode, the phase velocity is the speed of sound in the medium. At frequencies below the cutoff frequency of the first higher mode only the fundamental plane wave mode propagates without attenuation.

As the frequency is increased above the cutoff frequency of the first higher mode, the plane wave mode continues to propagate together with the first higher mode.

The phase velocity of the  $j$ th mode is

$$v_p = \frac{\omega}{k} = \frac{c}{\sqrt{1 - \left(\frac{c\gamma_j}{\omega}\right)^2}} . \quad (4.1.9)$$

and the group velocity for a group of waves centered about frequency  $\omega$  is

$$v_g = \frac{\partial\omega}{\partial k} = c \sqrt{1 - \left(\frac{c\gamma_j}{\omega}\right)^2} = \frac{c^2}{v_p} . \quad (4.1.10)$$

This velocity is less than  $c$  for frequencies above cutoff.

For a waveguide of circular cross section of radius  $R$ , the transverse eigenfunctions and eigenvalues of Eq. (4.1.3) are (Morse and Ingard, 1968)

$$\Psi_{m,n} = \frac{\cos}{\sin}(m\phi) J_m\left(\frac{\pi w r}{R}\right), \quad (4.1.11)$$

$$\gamma_{m,n} = \frac{\pi w}{R}, \quad (4.1.12)$$

where  $r$  and  $\phi$  are the polar coordinates about the central axis of the cylinder and where each pair of subscripts  $m, n$  defines a wave mode propagating in the waveguide. The subscript  $m$  indicates the number of nodal planes while the subscript  $n$  indicates the number of nodal cylinders. The alternative possibilities of using cosine or sine functions express the fact that the non axially symmetric modes are degenerate.

For each integer value of  $m$  there exist a set of values  $w$  which satisfy the boundary condition

$$J'_m(\pi w) = 0. \quad (4.1.13)$$

The solutions  $w$  which satisfy this condition are denoted as  $w = \alpha_{mn}$ . The plane wave mode corresponds to  $\alpha_{0,0} = 0$ ,  $J_0(\pi\alpha_{0,0}) = 1$ . From Eq. (4.1.12), the cutoff frequency of the  $(m,n)$ th mode is  $\alpha_{m,n}c/2R$  Hz.

The first mode above the plane wave mode is the  $(1,0)$  mode. This mode has one nodal plane extending radially out from the axis and no nodal circles. Since the axial velocity distribution is proportional to  $J_1(\pi\alpha_{1,0}/R)\cos(\phi)$ , the magnitude of the axial velocity along a line transverse to the nodal plane is 0 at the node

( $\phi = \pm\pi/2$ ) and a maximum at  $r=R$ . However, the axial velocities in the two halves of the waveguide are opposite in phase. This dipole mode is the dominant mode excited when the cylindrical waveguide is driven above cutoff with two speakers in an anti-symmetric push-pull configuration.

Generally the wavenumber  $k$  may have real and imaginary parts and we can write

$$k = \frac{2\pi}{\lambda_j} + i\pi\eta_j, \quad (4.1.14)$$

where  $\lambda_j$  is the wavelength along the axis of the waveguide of the  $j$ th mode and  $\eta_j$  is an attenuation factor. The sources of the attenuation are viscous and thermal losses at the duct walls as well as losses due to the acoustic admittance of the boundary surface. For a plane wave mode the attenuation due to thermoviscous losses is (Landau and Lifshits, 1959)

$$\eta_{0,0} = \frac{\sqrt{\omega\nu}}{\sqrt{2}Rc} \left( 1 + \sqrt{Pr}(\xi - 1) \right), \quad (4.1.15)$$

where  $\nu$  is the kinematic viscosity coefficient,  $Pr$  is the Prantl number, and  $\xi$  is the ratio of specific heats. An expression for the attenuation of the higher order propagating mode (1,0) as measured along the  $z$  axis is

$$\eta_{1,0} = \frac{\sqrt{\omega\nu}}{\sqrt{2}Rc} \left( \frac{c_p}{c \left[ 1 - (1/\pi\alpha_{10})^2 \right]} + \sqrt{Pr}(\xi - 1) \right). \quad (4.1.16)$$

The modification of the term above from its form in (4.1.15) can be understood by recognizing that the distance traveled by the wavefronts in the direction of their wavevectors is  $(c_p/c)$  times greater than the distance measured along the  $z$  axis. Because of the circular geometry the wavefronts are not straight. This effect is represented by the factor  $[1-(1/\pi\alpha_{10})^2]$ . Thus, the viscous losses are multiplied by  $(c_p/c[1-(1/\pi\alpha_{10})^2])$ . The contribution due to thermal losses remains the same because they are independent of the shear component of the velocity.

The distance at which the pressure field decreases by a factor  $e^{-1}$ , the e folding distance, is the inverse of the expression (4.1.16). It approaches 0 as the frequency approaches the mode's cutoff frequency, it has a maximum when  $\omega / c\gamma_{1,0}$  is approximately equal to  $3^{1/2}$ , and goes as  $\omega^{-1/2}$  for high frequencies.

## 2. THE NONLINEAR COEFFICIENT

The combined effects of nonlinearity and dispersion may force a single wavetrain to split into two separate wavetrains moving with unequal velocities. A calculation of the magnitude of the nonlinear coefficient is thus required to determine whether the effect is measurable for the specific case of the (1,0) cylindrical waveguide mode.

A general expression for the nonlinear coefficient for the wavenumber  $k_2$  has been obtained by Keller and Millman (1970). They consider the effect of a small finite amplitude sound wave propagating in a rigid cylindrical waveguide. A perturbation method is used by expanding the velocity potential  $\Phi$  and the

pressure  $p$  in powers of the dimensionless amplitude  $\varepsilon$  to solve the equations of fluid dynamics.

Specifically, consider the Bernoulli equation

$$\frac{\partial \Phi}{\partial t} + \frac{1}{2}(\nabla \Phi)^2 + \int_{p^{(0)}}^p \frac{dp}{\rho(p)} = 0, \quad (4.2.1)$$

and the continuity equation

$$p_p[\rho(p)] \nabla^2 \Phi - \frac{\partial^2 \Phi}{\partial t^2} = 2 \nabla \Phi \cdot \nabla \left( \frac{\partial \Phi}{\partial t} \right) + \frac{1}{2} (\nabla \Phi \cdot \nabla) (\nabla \Phi)^2, \quad (4.2.2)$$

where  $\Phi$  is the velocity potential,  $p$  is the pressure  $\rho(p)$  is the density,  $p^{(0)}$  is a constant and  $p_p$  is the derivative of the pressure with respect to the density.

Equations (4.2.1) and (4.2.2) must be supplemented with the boundary condition

$$\frac{\partial \Phi}{\partial n} = 0, \quad (4.2.3)$$

corresponding to the vanishing of the normal component of the velocity at the waveguide perimeter.

Regarding the frequency  $\omega$  as given and  $k$  as unknown and taking the  $z$  axis as parallel to the waveguide axis, solutions of the form

$$\Phi = \Phi(x, y, kz - \omega t), \quad p = p(x, y, kz - \omega t), \quad (4.2.4)$$

are sought.

Introducing the variable change  $z' = kz$  and  $t' = \omega t$  and then dropping the primes from the resulting equations allows us to rewrite Eqs. (4.2.1) and (4.2.2) in the form

$$\omega \frac{\partial \Phi}{\partial t} + \frac{1}{2} \left( \left( \frac{\partial \Phi}{\partial x} \right)^2 + \left( \frac{\partial \Phi}{\partial y} \right)^2 + k^2 \left( \frac{\partial \Phi}{\partial z} \right)^2 \right) + \int_{p^{(0)}}^p \frac{dp}{\rho(p)} = 0, \quad (4.2.5)$$

$$p_p[\rho(p)] \left( \frac{\partial^2 \Phi}{\partial x^2} + \frac{\partial^2 \Phi}{\partial y^2} + k^2 \frac{\partial^2 \Phi}{\partial z^2} \right) - \omega^2 \frac{\partial^2 \Phi}{\partial t^2} =$$

$$\frac{1}{2} \left( 2\omega \frac{\partial}{\partial t} + \frac{\partial \Phi}{\partial x} \frac{\partial}{\partial x} + \frac{\partial \Phi}{\partial y} \frac{\partial}{\partial y} + k^2 \frac{\partial \Phi}{\partial z} \frac{\partial}{\partial z} \right) \left( \frac{\partial^2 \Phi}{\partial x^2} + \frac{\partial^2 \Phi}{\partial y^2} + k^2 \frac{\partial^2 \Phi}{\partial z^2} \right), \quad (4.2.6)$$

where

$$\Phi(x, y, z - t + 2\pi) = \Phi(x, y, z - t),$$

$$p(x, y, z - t + 2\pi) = p(x, y, z - t). \quad (4.2.7)$$

The Taylor expansion of  $\Phi$ ,  $p$ , and  $k$  in terms of  $\varepsilon$  can be obtained as follows

$$\Phi_n(x, y, z - t, \varepsilon) = \varepsilon \Phi_n^{(1)} + \frac{\varepsilon^2}{2} \Phi_n^{(2)} + \dots, \quad (4.2.8)$$

$$p_n(x, y, z - t, \varepsilon) = p^{(0)} + \varepsilon p_n^{(1)} + \frac{\varepsilon^2}{2} p_n^{(2)} + \dots, \quad (4.2.9)$$

$$k_n(\varepsilon) = k_n^{(0)} + \varepsilon k_n^{(1)} + \frac{\varepsilon^2}{2} k_n^{(2)} + \dots, \quad (4.2.10)$$

where the superscripts denote the  $j$ th derivative with respect to  $\varepsilon$  and the subscript denotes the propagating mode. The justification for Eq. (4.2.10) is that the Taylor expansions of  $\Phi$  and  $p$  in terms of  $\varepsilon$  do not exist unless  $k$  also depends on  $\varepsilon$ .



Keller and Millman (1970) insert Eqs. (4.2.8) - (4.2.10) into Eqs. (4.2.5) and (4.2.6). They show that  $k_n^{(1)} = 0$  and obtain the following general expression for the coefficient  $k_n^{(2)}$

$$k_n^{(2)} = \frac{1}{2c^2 k_n^{(0)}} \int (\omega \nabla_T \beta_n \cdot \nabla_T \Psi_n - \frac{3}{2} \Psi_{nxi} \Psi_{nxj} \Psi_{nxi} - \left\{ \left[ k_n^{(0)} \right]^2 + h \right\} \Psi_n |\nabla_T \Psi_n|^2 - 2\omega \left\{ \left[ k_n^{(0)} \right]^2 + 2h \right\} \beta_n \Psi_n + q_n \Psi_n^3) \Psi_n dx dy . \quad (4.2.11)$$

where  $c$  is the speed of sound in the medium,  $k_n^{(0)}$  is the linear wavenumber for which  $\left[ k_n^{(0)} \right]^2 = \frac{\omega^2}{c^2} - \gamma_n^2$  ( $\gamma_n$  is the eigenvalue of the wave equation (4.1.3) and  $\Psi_n$  is the corresponding eigenfunction),  $\nabla_T$  is the transverse Laplacian,  $\beta_n$  is determined by solutions to

$$\left( \nabla_T^2 + 4\gamma_n^2 \right) \beta_n = \left( \frac{2\omega}{c^2} \right) \left\{ |\nabla_T \Psi_n|^2 - \left( \left[ k_n^{(0)} \right]^2 + 2h \right) \Psi_n^2 \right\} , \quad (4.2.12)$$

and

$$\Psi_{nxi} \Psi_{nxj} \Psi_{nxi} = \left( \frac{\partial \Psi_n}{\partial x} \right)^2 \frac{\partial^2 \Psi_n}{\partial x^2} + 2 \frac{\partial \Psi_n}{\partial x} \frac{\partial \Psi_n}{\partial y} \frac{\partial^2 \Psi_n}{\partial x \partial y} + \left( \frac{\partial \Psi_n}{\partial y} \right)^2 \frac{\partial^2 \Psi_n}{\partial y^2} . \quad (4.2.13)$$

For an ideal gas equation of state  $p(\rho) = A\rho^\xi$

$$h = (\xi - 1) \frac{\omega^2}{4c^2}, \quad (4.2.14)$$

and

$$q_n = \frac{1}{2} \left( k_n^{(0)} \right)^4 + \frac{(\xi - 1)(2\xi - 1)\omega^4}{4c^4} + \frac{(\xi - 1)\omega^2}{c^2} \left\{ \left( k_n^{(0)} \right)^2 - \frac{\gamma_n^2}{4} \right\}. \quad (4.2.15)$$

We now specialize these results to the case of the first non-axially symmetric mode propagating in a cylindrical waveguide of radius  $R$ . From Eq. (4.1.11) the normalized solution of the full wave equation for this mode is

$$\Psi_{1,0} = \frac{\sqrt{2\pi}\alpha_{1,0} \cos(\phi) J_1 \left( \frac{\pi\alpha_{1,0}r}{R} \right)}{R J_1(\pi\alpha_{1,0}) \sqrt{(\pi\alpha_{1,0})^2 - 1}}. \quad (4.2.16)$$

This mode is doubly-degenerate and even when an external drive breaks the symmetry, nonlinearities resonantly couple the two eigenmodes. However, because a real waveguide is not perfectly circular the degeneracy is removed and the frequency difference is a monotonic function of the eccentricity. Thus we will assume a nondegenerate solution of the form (4.2.16) and determine the nonlinear coefficient (4.2.11) accordingly.

To obtain an expression for  $\beta_{1,0}$  we insert (4.2.16) into (4.2.12) and transform to polar coordinates. The right hand side of the inhomogeneous Eq. (4.2.12) is of the form  $F(r) + H(r) \cos(2\phi)$ , where  $F(r)$  and  $H(r)$  are in terms of products of

two Bessel functions. The solution of (4.2.12) satisfying the boundary condition (4.2.3), which becomes  $\beta_{1,0}'(R) = 0$ , is

$$\beta_{1,0}(r) = \int_0^R G_0(r,s)F(s)sds + \cos(2\phi) \int_0^R G_2(r,s)H(s)sds . \quad (4.2.17)$$

Here, the Green's functions  $G_m(r,s)$  are given by

$$G_m(r,s) = \frac{\pi}{2} \frac{J_m(2\pi\alpha_{1,0}r_</R)}{J_m'(2\pi\alpha_{1,0})} \quad (4.2.18)$$

$$\times [J_m(2\pi\alpha_{1,0}r_>/R)N_m'(2\pi\alpha_{1,0}) - N_m(2\pi\alpha_{1,0}r_>/R)J_m'(2\pi\alpha_{1,0})] .$$

where  $N_m$  is the Neumann function of order  $m$ , and  $r_>$  ( $r_<$ ) stands for the greater (smaller) of  $r$  and  $s$ . Using (4.2.14)-(4.2.18) we obtain for  $k_{1,0}^{(2)}$  the following

$$k_{1,0}^{(2)}(\omega) = \left( \frac{\sqrt{2\pi\alpha_{1,0}}}{RJ_1(\pi\alpha_{1,0})\sqrt{(\pi\alpha_{1,0})^2 - 1}} \right)^4 \quad (4.2.19)$$

$$\frac{\pi^2\alpha_{1,0}^2}{2c^2R^2k_{1,0}^{(0)}} \{ 0.305 + 0.38x^2 - 1.463x^4 + 0.371x^6 \} ,$$

where  $x = \omega R/(c\pi\alpha_{1,0})$  is the ratio of the frequency to the cutoff frequency. The expression (4.2.19) has meaning for  $x > 1$ . It is negative for  $1 < x \leq 1.897$  and becomes positive for frequencies larger than 1.897 times bigger than the cutoff frequency.

The wavenumber is the result of developments in powers of  $\varepsilon$  which is the amplitude of the linearized solution. In terms of the ratio of the acoustic pressure to the ambient pressure we obtain

$$k_{1,0} = \left( \frac{\omega^2}{c^2} - \frac{(\pi\alpha_{1,0})^2}{R^2} \right)^{1/2} + \frac{c^4}{2} \left( \frac{RJ_1(\pi\alpha_{1,0})\sqrt{(\pi\alpha_{1,0})^2 - 1}}{\sqrt{2}\pi\alpha_{1,0}\xi\omega} \right)^2 k_{1,0}^{(2)} \left( \frac{p}{p_0} \right)^2. \quad (4.2.20)$$

The propagation constant  $k_{1,0}$  depends upon amplitude. It is less than the linear value for frequencies between the cutoff frequency and 1.897 times the cutoff frequency. According to the physical arguments presented in the Chapter 1, a modulation of a wavetrain will be stable and an initial disturbance will split into two disturbances moving with different group velocities. On the other hand, for frequencies greater than 1.897 times the cutoff frequency the phase velocity is a decreasing function of amplitude and modulations of a wavetrain will become unstable to the formation of solitons.

The formalism developed in the previous chapters relies on the determination of the nonlinear coefficient  $\omega_2$ . Equation (4.2.20) gives the frequency dependence of the propagation constant  $k_{1,0}$ . Thus, we can solve implicitly for the frequency as a function of wavenumber  $k = k_{1,0}$ . If we set  $\omega = \omega_0 + \omega_2(p/p_0)^2$ , it can be shown that

$$\omega_2(k) = -\omega'_0(k) \frac{c^4}{2} \left( \frac{RJ_1(\pi\alpha_{1,0})\sqrt{(\pi\alpha_{1,0})^2 - 1}}{\sqrt{2}\pi\alpha_{1,0}\xi\omega_0(k)} \right)^2 k_{1,0}^{(2)}(\omega_0(k)) \left( \frac{p}{p_0} \right)^2, \quad (4.2.21)$$

where

$$\omega_0(k) = c \sqrt{\left(\frac{\pi \alpha_{1,0}}{R}\right)^2 + k^2} \quad (4.2.22)$$

is the linear dispersion relation and  $\omega_0'$  is the linear group velocity at the wavenumber  $k$ .

### 3. EXPERIMENTAL CONSEQUENCES

For a fixed frequency, Eq. (4.2.20) predicts that the wavelength of a nonlinear wave changes with amplitude. It increases with amplitude for frequencies less than 1.897 times the cutoff frequency and decreases with amplitude for frequencies that are larger than 1.897 times the cutoff frequency. The mode is modulationally stable in the former case and we will restrict our analysis to this frequency range.

The effect of increasing the wavelength with amplitude can be determined experimentally by measuring the relative phase between two points. If the distance  $d$  between two points is less than the wavelength

$$\frac{\Delta \phi}{\phi} = \frac{\Delta k}{k} \quad , \quad (4.3.1)$$

where  $\Delta\phi$  is the change in phase difference  $\phi$  between two points due to a change in amplitude, and  $\Delta k = k_{1,0} - k_{1,0}^{(0)}$ . The effect can be magnified if the distance between the two points several wavelengths apart. In this case

$$\frac{\Delta\phi}{\phi + 2\pi N} = \frac{\Delta k}{k} \quad (4.3.2)$$

where  $N$  is the integer number of wavelengths in the distance  $d$  between the two points. The slope of the measured relative phase between two points as function of the square of the amplitude will thus yield an experimental value of the nonlinear coefficient. This value in turn, can be used to determine the separation in time as a function of distance of the split pulses.

To determine the difference of the times of arrival at a given location of the two disturbances that result from the splitting of an initial disturbance we can use Eq. (3.1.4). In terms of the ratio  $p/p_0$  of the acoustic pressure to the ambient pressure, (3.1.4) becomes

$$\frac{dz}{dt} = \omega_0'(k) \pm \left\{ \omega_2(k) \omega_0''(k) \right\}^{1/2} \left( \frac{p}{p_0} \right) \quad (4.3.3)$$

A finite extent modulation of a nonlinear wavetrain generated at a source at  $z=0$  will split into two disturbances that arrive at a distance  $z$  with a time difference given by

$$\Delta t_n(z) = z \frac{2(\omega_0'' \omega_2)^{1/2}}{(\omega_0')^2} \left( \frac{p}{p_0} \right) \quad (4.3.4)$$

In order to determine if this effect is observable, we must also determine if the time spread due to dispersion is smaller than the time due to splitting.

The average velocity of a smooth pulse or a finite wavetrain that does not cut off too violently is the group velocity  $v_g = d\omega_0/dk = \omega_0'$ . Due to dispersion the pulse spreads because different frequency components move with different phase velocities. The spreading of the pulse can be accounted for by noting that a pulse with initial temporal width  $\Delta t_0$  must have an inherent spread of frequencies  $\Delta\omega \sim (1/\Delta t_0)$ . This means that the group velocity spread is of the order

$$\Delta v_g \sim \frac{\omega_0''}{\omega_0'} \Delta\omega \sim \frac{\omega_0''}{\omega_0' \Delta t_0} \quad , \quad (4.3.5)$$

which at a point  $z$  implies a spread in time of the order of  $\Delta v_g z / (\omega_0')^2$ . Because the uncertainty in time is the square root of the sum of squares the width  $\Delta t(z)$  at location  $z$  is

$$\Delta t_d(z) \approx \sqrt{(\Delta t_0)^2 + \left( \frac{\omega_0'' z}{\omega_0'^3 \Delta t_0} \right)^2} \quad . \quad (4.3.6)$$

The expression for  $\Delta t(z)$  shows that in a medium with dispersion a narrow pulse spreads rapidly because of its broad spectrum in frequencies. Thus the criterion for a small change in shape is that  $\omega_0'^2 \Delta t_0 \gg \omega_0''$ .

Thus, for the splitting to be observable *for all distances* we require that

$$2\Delta t_0 \omega_0' \left( \frac{\omega_2''}{\omega_0''} \right)^{1/2} \frac{p}{p_0} > 1 \quad (4.3.7)$$

For a 10 ms disturbance superimposed on a signal with a frequency 10% higher than the cutoff frequency the minimum ratio of acoustic pressure to ambient pressure is 0.005, or 148 dB (re 20  $\mu$ Pa).

The estimate (4.3.7) guaranties that the curves (4.3.4) and (4.3.6) do not intersect. For low intensity levels the two curves intersect. However, it should still be possible to observe the splitting of a pulse into two pulses for distances less than the distance given by the real solution to

$$(\Delta t_0)^2 + \left( \frac{\omega_0'' z}{\omega_0'^3 \Delta t_0} \right)^2 = \left( \Delta t_0 + z \frac{2(\omega_0'' \omega_2')^{1/2}}{(\omega_0')^2} \left( \frac{p}{p_0} \right) \right)^2, \quad (4.3.8)$$

provided the value  $\Delta t_n$  given by (4.3.4) is within the limits of instrumental resolution. Spreading due to dispersion will dominate for distances larger than the distance determined by the real solution of (4.3.6). However, even when the splitting of a disturbance into two cannot be observed, the effects of the double group velocity will be to spread a given pulse beyond the values predicted by linear dispersion.



## CHAPTER 5. EXPERIMENTAL RESULTS

In this chapter we discuss the experimental results related to propagation of the (1,0) cylindrical waveguide mode in the frequency regime for which the mode is modulationally stable. We briefly describe the experimental apparatus used in our experimental investigations. The experimental results include measurements of the (1,0) mode linear cut off frequency, group velocity, and attenuation constants for frequencies above the cutoff frequency. From frequency response measurements we also determine the relative amplitudes of the plane wave and dipole modes. Also, we measure the spreading of a low amplitude acoustic pulse. Finally, investigations of nonlinear effects including the determination of the nonlinear coefficient at 4200 Hz and preliminary time domain observations of group velocity splitting in amplitude modulated and in pulse modulated acoustic waves are presented.

### 1. EXPERIMENTAL APPARATUS

The experimental apparatus is a traveling wave tube made of an extruded aluminum pipe of average inner diameter 1.957 inches, outer diameter 2.377 inches, length 70 feet, which consist of seven 10 foot sections joined by collars and flanges. An anechoic end termination made of steel wool with a tapered density distribution spans the length of the 7th section. Absorber and junction

reflection amplitudes are typically -40dB down for frequencies between 1kHz and 4kHz (Dorff, 1991).

Each of the first six sections of pipe have 4 microphone ports which accommodate ENDEVCO series 8510B piezoresistive pressure transducers. The ports have a uniform spacing of 2.5 feet. An additional port was added directly below the 2nd port in the 5th section (from the drivers' end of the pipe). This port adds the capability of instrumentally eliminating the detection of the plane wave mode by connecting the microphones with opposite polarity and adding their output.

Two JBL model 2445H compression drivers were mounted at one end of the wave tube via a two-to-one adapter. The first microphone port is at a distance of 0.83 m from the drivers. The drivers are titanium diaphragm drivers rated at 100 watts from 500 Hz to 1000 Hz and 150 watts above 1 kHz.

A two-to-one adapter was designed such that the *drivers could be mounted* directly opposed (Fig. 5.1). The inner diameter of the adapter was machined to a diameter of 1.975 inches to match the inner end diameter of the wave tube. The speakers were mounted flat to the adapter onto rectangular attachment flanges. A 2 inch to 1 inch tapered bore made through the attachment flanges and the adapter connected the 2 inch driver opening to the 1.975 inch diameter waveguide opening.

In this configuration, the drivers operate in push - pull when driven 180 degrees out of phase. The plane wave mode can in principle be nulled by adjusting the amplified signal to each driver. In this manner, at frequencies above cutoff the (1,0) mode is the main propagating mode.

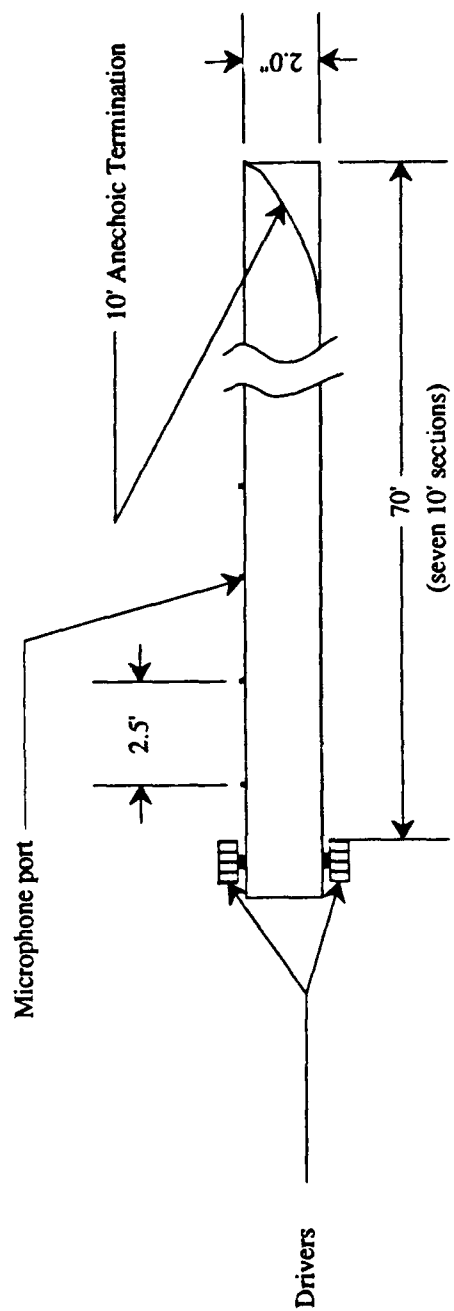


**Fig 5.1 Traveling Wave Tube**

## **2. EXPERIMENTAL RESULTS**

### **a) Frequency Response**

In an acoustic waveguide the plane wave mode propagates at all frequencies. Although the experimental procedure calls for nulling the plane wave component of the acoustic field, the frequency responses of the drivers are not identical. Therefore, even if the plane wave component is nulled at one frequency, it may not be so for other frequencies in the sweep.

The role played by the plane wave field was investigated by taking frequency response measurements with a swept sine source at the first port 0.83 m from the drivers' end and at each alternate port. The frequency span of the sweep is from 3900 to 4400 Hz, with a resolution of 401 points per sweep. The plane wave component was nulled at 3900 Hz.

To investigate the effects that the presence of a plane wave might have in the dipole field, we obtained frequency responses measured at the double ports located at 13.79 m from the drivers' end. The double port arrangement allows measurements to be obtained by the output of a single microphone as well as the output of the sum of the two microphones with the same and with opposite polarities.

The frequency response measured from a single microphone is the superposition of a plane wave and a dipole field. For a given frequency, the corresponding wavelengths of the two modes are not the same. Consequently, the relative phase of the corresponding acoustic pressure is a function of frequency. Thus we should expect that the interference between the two fields

at a given point be reflected in the frequency response at this point. Fig. 5.2a shows a sinusoidal variation of the amplitude as a function of frequency.

Fig. 5.2b shows the output at the dual port of two microphones with the same polarity. In this arrangement the dipole field is canceled and the output corresponds to a frequency response of the plane wave. The inconsistency in the amplitudes for the frequency responses of Fig. 5.a as compared to that in Figs. 5.b,c is due to the difference in the microphone gain used to obtain these signals. The microphone gain in Fig. 5.a is 500 while the gain used to obtain Figs. 5.b,c is 10k. Note that for frequencies above 4050 Hz, the amplitude decreases with increasing frequency. In Figs. 5.2a,b the frequency response abruptly dips at 4030.2 Hz which corresponds to the cutoff frequency for the (1,0) mode.

Alternatively, Fig. 5.2c shows the output at the dual port of two microphones with opposite polarity. In this arrangement the plane wave field is canceled and the output corresponds to the frequency response of the (1,0) mode dipole field. For frequencies greater than 4200 Hz, the frequency response is essentially flat.

A comparison of Figs. 5.2a,b&c leads us to the conclusion that interference is occurring between the plane wave and the (1,0) mode. As shown in Figs. 5.2b&c the plane wave mode is observed to be between 9 and 25 dB down from the dipole mode for frequencies above the cutoff.

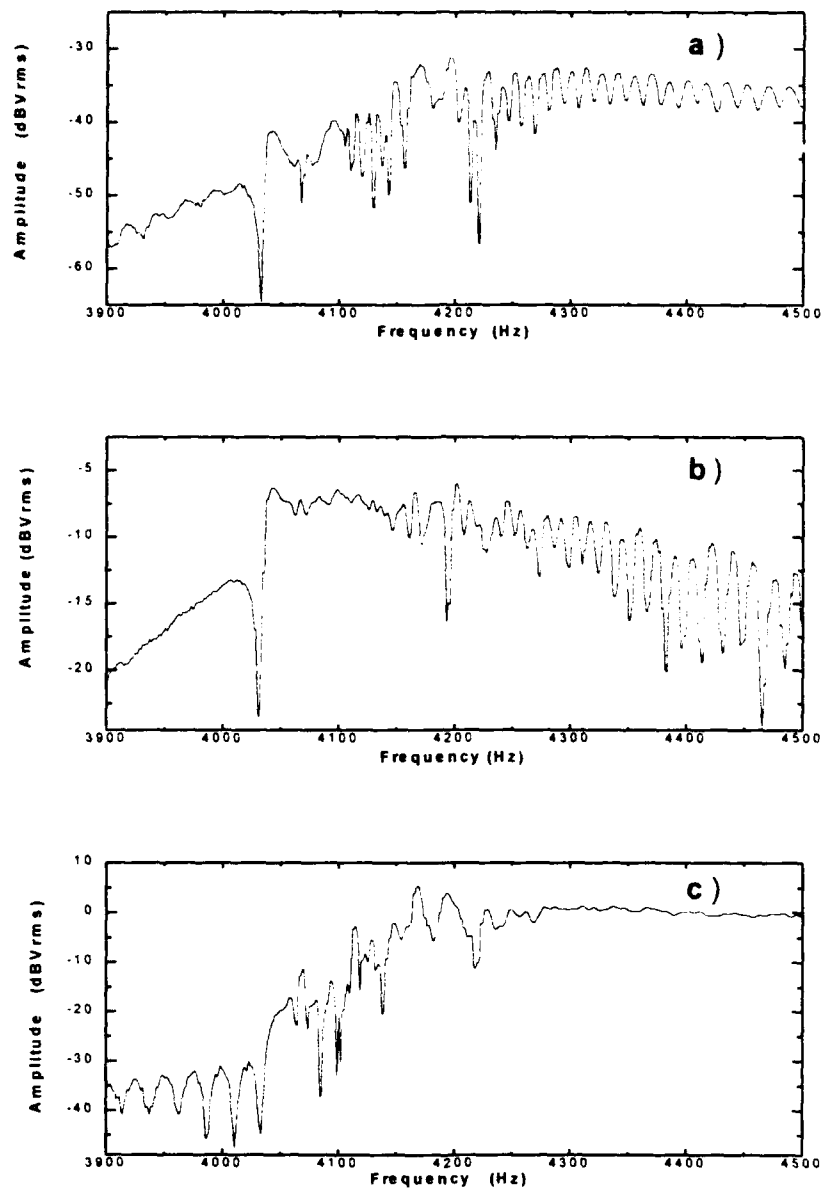


**Fig. 5.2** Frequency response of the traveling wave tube measured at the dual port 13.79 m from the drivers. a) Output from single microphone. Mike gain is 500. b) Output from two microphones with equal polarity c) Output from two microphones with opposite polarity. Mike gain for b,c is 10k.

### **b) Attenuation Constant**

From the frequency response at each port we obtained microphone signal amplitudes for 401 frequencies between 3900 Hz and 4400 Hz. A matrix was constructed from this data. The rows of the matrix contain the signal amplitudes at fixed frequency for 14 microphone port locations. The columns list signal amplitudes at a fixed location for 401 separate frequencies between 3900 and 4400 Hz. Using this matrix, we obtained plots of the amplitude versus distance for each frequency. From an exponential fit performed on the data, we obtained the attenuation constants for frequencies between 4050 and 4400 Hz.

Fig. 5.3a is a plot of the  $e^{-1}$  folding distance as a function of frequency. The attenuation constant corresponds to the inverse of this distance. The plot of this data shows irregularly high and low  $e^{-1}$  folding distances between the frequencies 4100 to 4200 Hz. As suggested by Fig. 5.2 the variation in the  $e^{-1}$  folding distance between these frequencies is due to the rapid variations in the frequency response at the different ports between these frequencies. That is, the frequency corresponding to a peak at one port may not necessarily correspond to a peak at another port. This observation is supported by the fact that variation in the  $e^{-1}$  folding distances is not observed at frequencies where the amplitude of the frequency response is relatively flat.

In Fig. 5.3b we have removed the extreme high and low attenuation factors in the frequency range 4100 to 4200 Hz. The solid curve in Fig. 5.3b, obtained from Eq. (4.1.15), corresponds to the predicted attenuation length due to thermoviscous losses. Excellent agreement between theory and experiment is observed up to 4300 Hz where pipe radiation losses possibly become important.

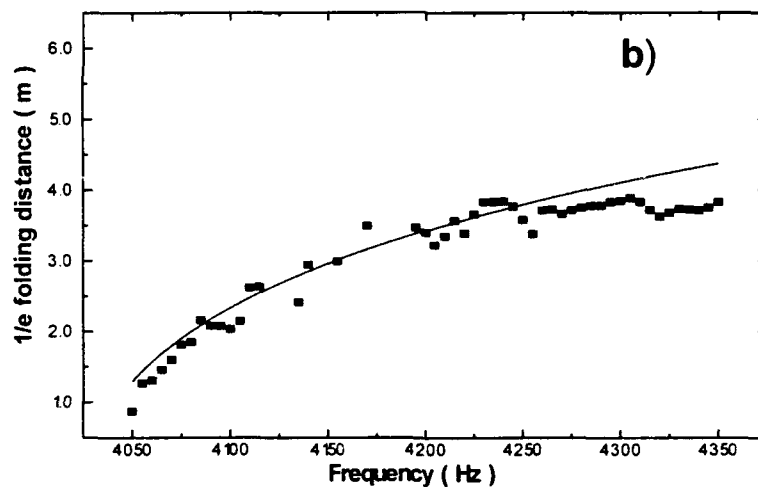
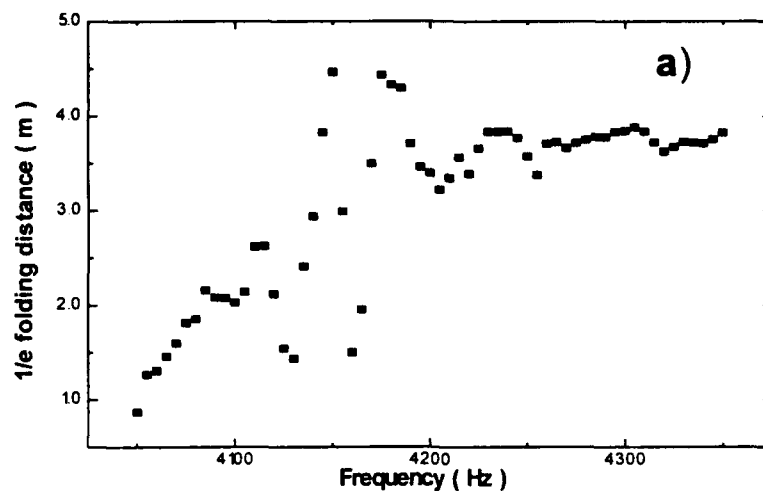


**Fig. 5.3** Plot of the 1/e folding distance as a function of frequency. The extreme high and low variations in (a) have been removed in (b). The solid line corresponds to theory.



### c) Group Velocity Measurements

The frequency response plots of Fig. 5.2 show a change in behavior for frequencies above the cutoff frequency of 4030.2 Hz. According to the theory, when the drivers are in a push-pull configuration the dominant propagating mode is the (1,0) mode. For this mode, the group velocity depends on frequency according to the relation (4.1.10)

$$v_g = c \left( 1 - (\omega_c / \omega)^2 \right)^{1/2} \quad (5.2.1)$$

where  $\omega_c$  is the cut off frequency of the (1,0) mode. Thus for a fixed distance  $D$ , the time of travel  $\Delta t$  is

$$(1/\Delta t)^2 = c^2/D^2 \left\{ 1 - \omega_c^2 (1/\omega^2) \right\} \quad (5.2.2)$$

We made measurements of the time of flight of a 100 cycle burst with carrier frequencies above cutoff. The envelope was sinusoidal. The time delay measurements were made at a single port and a fixed location 13.79 m from the drivers on a Nicolet Oscilloscope triggered externally from the driver signal. Time delays were measured from the time of trigger to the time of half maximum signal amplitude for five frequencies (Coppens, 1966). Fig. 5.4 shows the plot of the resulting data. As predicted from (5.2.2) there is a linear relationship between the inverse of the square of the time delay ( $1/\Delta t^2$ ) and the inverse of the square of the frequency ( $1/f^2$ ). A least square fit of the data yields a cutoff frequency of 4040 Hz. This result is within 0.2% of the value obtained from the frequency response data. The experimentally obtained value for the speed of sound is 338.7 m/s.

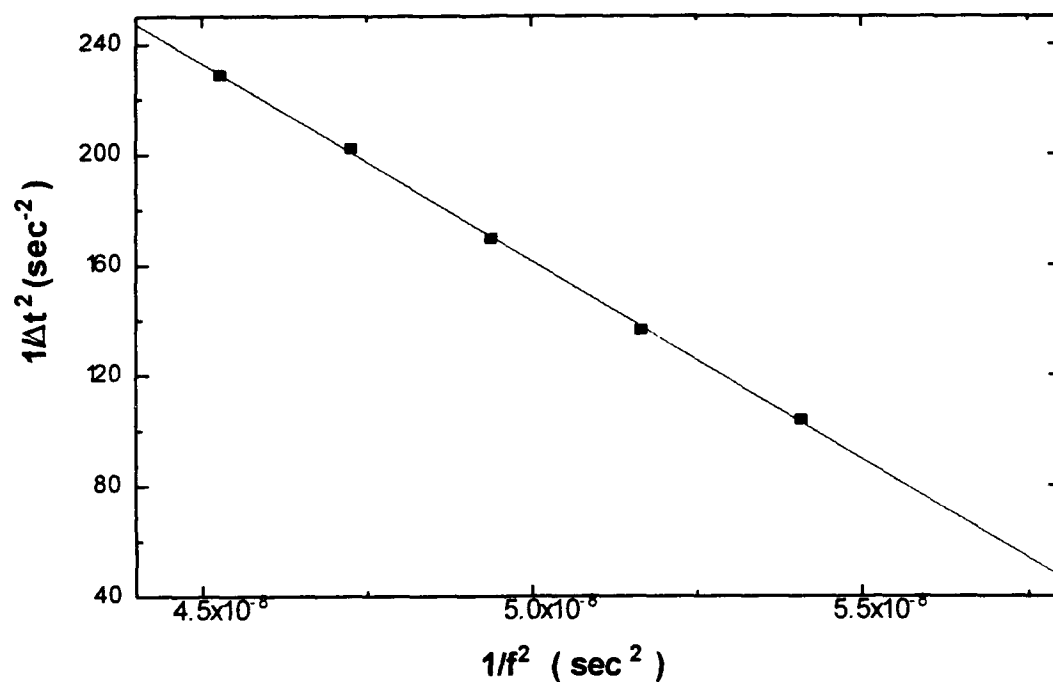


**Fig. 5.4** Group velocity measurements. The graph shows a linear dependence between the inverse of the square of the time delay and the inverse of the square of the frequency for the (1,0) mode for 5 frequencies above cutoff. Slope = 877.9 ; Intercept =  $-1.43 \times 10^{10}$ .

#### d) Measurements of Pulse Spreading

Equation (4.3.6) estimates the spreading of an acoustic pulse due to dispersion. This equation predicts that the spreading is significant only at distances much greater than the length of our waveguide or for frequencies very close to cutoff. Specifically, predictions for the spreading of a 21.7 ms pulse propagating a distance of 7.69 m range from 0.002 ms for a 4.6 kHz signal to 0.1 ms for a 4.2 kHz signal. These times are within the instrumental uncertainty of the Nicolet oscilloscope.

In order to verify the prediction that the spreading due to dispersion was negligible, we analyzed the spreading of a low amplitude N cycle pulse of 21.7 ms duration. The carrier was modulated to obtain a smooth sinusoid envelope. The number of cycles N was varied to keep the input pulse duration constant. Measurements of pulse spreading were made by measuring the total time duration of the pulse signals obtained at locations 0.83m and 7.69m from the drivers. Table 5.1 shows the measurements obtained for 5 frequencies.

Table 5.1

	4.6 kHz	4.5 kHz	4.4 kHz	4.3 kHz	4.2 kHz
	(ms)	(ms)	(ms)	(ms)	(ms)
0.0 m	21.5 ± .2	21.7 ± .2	21.7 ± .2	21.7 ± .2	21.7 ± .2
0.83 m	22.0 ± .4	24.0 ± .4	24.7 ± .4	25.5 ± .2	27.1 ± .2
7.69 m	21.6 ± .4	21.8 ± .4	22.0 ± .4	22.2 ± .4	

The data verify that for the propagation distances and frequencies measured the contribution to the spreading from dispersion is negligible.

The spreading of the pulse at 0.83 meters is apparently due to the fact that at this distance the plane wave has not yet unraveled from the center of the dipole mode pulse. That is, the microphone signal consists of a plane wave component as well as a dipole component where each travel with different velocities of propagation and therefore arrive at the microphone at different times. For example, in considering the data for the 4.4 kHz signal, the plane wave component arrives at the microphone in 2.45 ms. The dipole component arrives in 6.1 ms. The combined signal would therefore appear to be 3.6 ms longer than the input signal. Experimentally, the signal at the .83 meter location for 4.4 kHz is observed to be 3 ms longer than the input.

Signal distortion prevented a reliable measurement of the duration of the 4.2 kHz signal from the 7.69m location.

### e) Measurement of the Nonlinear Coefficient

As shown in Fig. 5.4, for frequencies above cutoff the mode is dispersive. For small but not infinitesimal amplitude, the dispersion relation for the (1,0) mode is of the form given by Eq. (2.2.1). According to this expression, for fixed frequency a change in the amplitude induces a change in wavelength of the mode. If the nonlinear coefficient is positive the changes in the wavenumber decrease linearly with the square of the amplitude. Thus, by measuring the relative phase between two points as a function of amplitude we can determine both the validity of Eq. (2.2.1) and the nonlinear coefficient.

Using a PAR 5210 lock-in amplifier we determined the amplitude of the acoustic field at 13.79 m from the drivers and the phase of this signal relative to a reference signal located at a distance of 9.98 m from the drivers. By varying the driver amplitude at a fixed frequency, in this case 4200 Hz, we obtained the relative phase between the two signals as a function of the amplitude squared. The plane wave component of the acoustic field was nulled at this frequency.

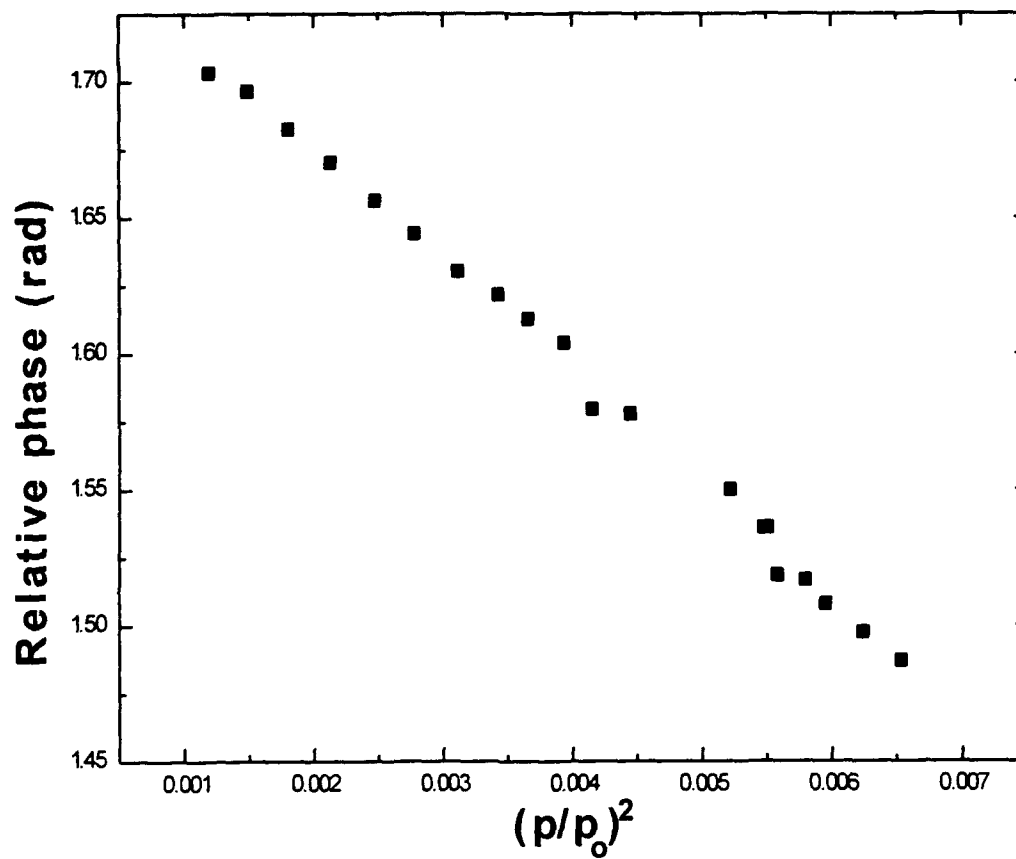
The data in Fig. 5.5 are in terms of the acoustic pressure at the source. A reasonable estimate of the amplitude at the source was obtained by multiplying the calibrated acoustic amplitude at 13.79 m by the inverse attenuation factor  $e^{13.79 / 3.39}$ , where 3.39 m is the 1/e folding distance of a (1,0) mode of frequency equal to 4200 Hz.

Fig. 5.5 shows a linear relation between the relative phase and the square of the acoustic amplitude at the source. In order to get an idea of the intensity levels used for this measurement, the pressure amplitude has been normalized to the atmospheric pressure. The plotted range varies between 150 dB and 170 dB (re 20  $\mu$ Pa). The nonlinear coefficient can be determined from using the

slope of the line and Eq. (4.3.2). For a frequency of 4200 Hz, the theoretical value predicted by Eq. (4.2.20) yields  $\Delta k = -12.58 (p/p_0)^2$ . In the span of 3.81 m, corresponding to the distance between the two ports there are 13 wavelegths. Thus we obtain

$$\frac{\Delta k}{k}(\varphi + 2\pi N) = -47.03 \left( \frac{p}{p_0} \right)^2 \quad (5.2.3)$$

The predicted slope is 12% bigger than the experimental value of - 41.36.



**Fig. 5.5** Plot of the relative phase versus the square of the normalized acoustic pressure at the source. Pressure amplitudes are normalized to 1 atmosphere.

### **f) Measurements of Group Velocity Splitting**

An initial disturbance superimposed on a signal with a frequency 10% higher than the cutoff frequency splits into two and the differential time of arrival is approximately  $30 z(p/p_0)$  ms at a distance  $z$  from the source (Eq. (4.3.4)).

Fig. 5.6 shows the microphone output on a Nicolet digital oscilloscope for three different locations and three different intensity levels.

The input signal is generated using 2 HP 3314 function generators. A 4500 Hz carrier is amplitude modulated by a 100 Hz inverted half-sine wave at 1 sec intervals. The first, second and third rows in Fig. 5.6 correspond to intensity levels of 140 dB, 144 dB, and 156 dB at the source, respectively. At 140 dB no apparent splitting of the negative pulse is observed up to the shown distance of 7.69, while the spreading of the pulse is noticeable. However at 144 dB and 156 dB the pulse undergoes spreading and a splitting becomes readily apparent for distances of 4.64 m and beyond.

We performed quantitative analysis of the signals displayed in Fig. 5.6. The procedure used consists of multiplying the data by the cosine of the carrier frequency, taking the Fast Fourier Transform (FFT) of the product and then filtering the modulus of the FFT to remove the high frequency components of the frequency spectrum. The inverse FFT of the filtered frequency spectrum is then taken to recover the signal modulation exclusively.

With this procedure we can determine the time spread of the pulse and the differential time of the split portions. Measurements were made from the waveform peaks. For a sound level of 140 dB a 10 ms pulse spreads into an 11.8 ms pulse at 4.64 m and into a 14.2 ms pulse at 7.69 m. Thus the delayed



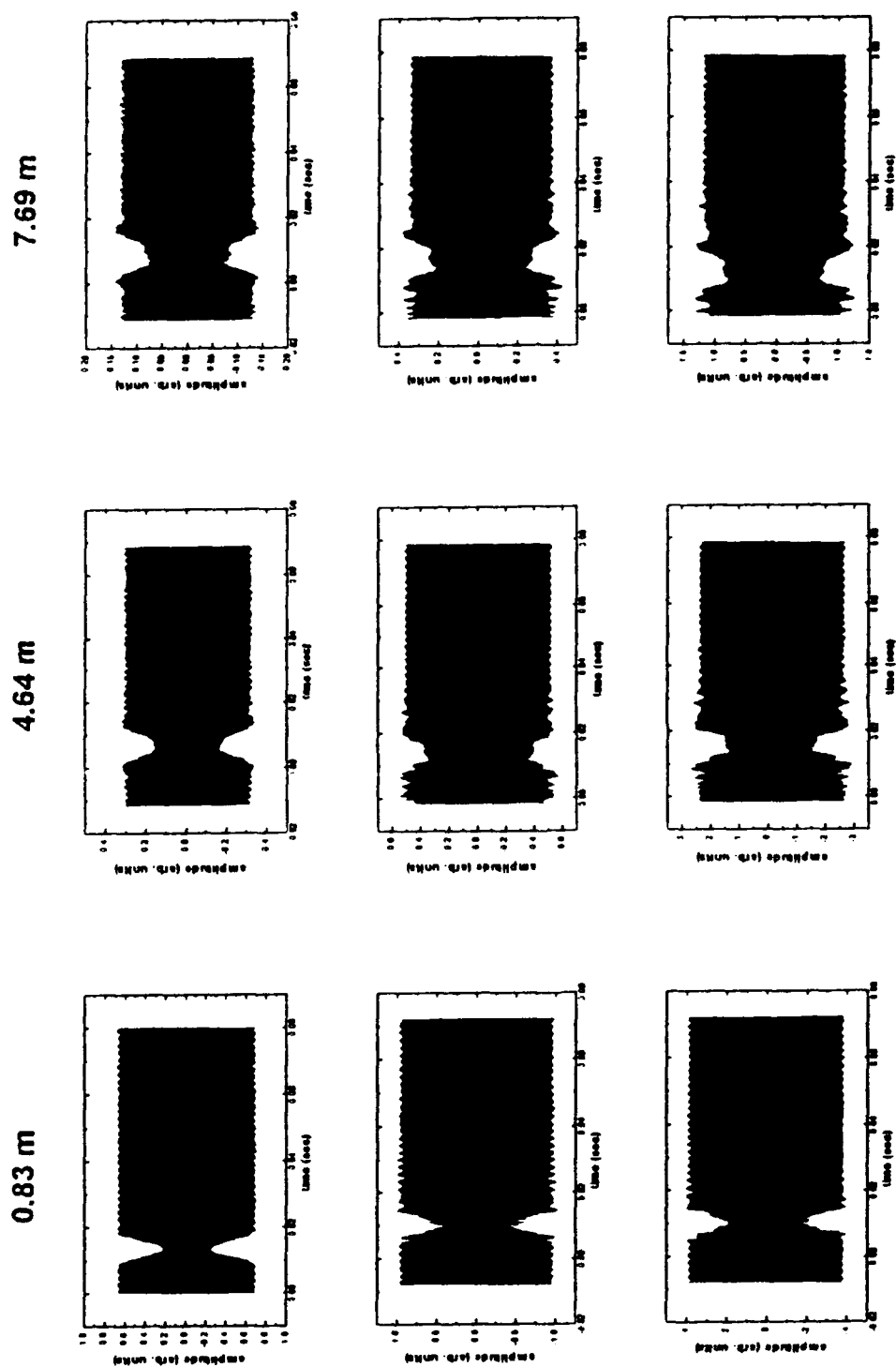


Fig 5.6 A 10 ms negative modulation at 1 sec intervals of a 4.5 kHz carrier measured at different locations. The first, second, and third rows correspond to 140 dB, 144 dB, and 156 dB at the source respectively.

time is 2.4 ms and it is not at all described by dispersion. Furthermore, at 10.73 m the pulse undergoes splitting where the difference between the two peaks is 5.5 ms.

Similarly, for an intensity of 144 dB the apparent spread of a 10 ms pulse at 4.64 m is 14.7 ms, while at 7.69 m the spread is 17.0 ms. This corresponds to a delay of 2.3 ms. The split pulses at these locations are 4.1 ms and 6.1 ms apart respectively. Remarkably there is a delay of 2 ms in the split pulses between these two locations. That is, the splitting the pulse occurs with a delay nearly equal to the differential spread.

Furthermore, a comparison of the 144 dB and the 156 dB signals at 7.69 m shows a significant increase in the time interval between two peaks of the modulation. Fig. 5.7 shows that for the lower amplitude signal, the time interval between the two most negative peaks of the modulation is 6.1 ms. For high amplitude the time interval between these same two peaks is 8.4 ms. The time delay is 2.3 ms verifying that the splitting increases as a function of amplitude. On the other hand, the 17 ms spread is the same for both amplitudes.

Using a single HP 3314 function generator in the N cycle mode, we generated a pulsed sine wave of 50 cycles with frequency 4.2 kHz. We varied the amplitude of the driver input signal and obtained time domain measurements of a microphone output signal at 10.74 m from the drivers. The envelope of the pulse was recovered using a procedure identical to that described above.

Fig. 5.8 shows the modulations of a 150 dB and a 178 dB bursts. The time intervals between the two marked peaks are 33.75 ms and 35.56 ms respectively. The time delay is 1.8 ms.

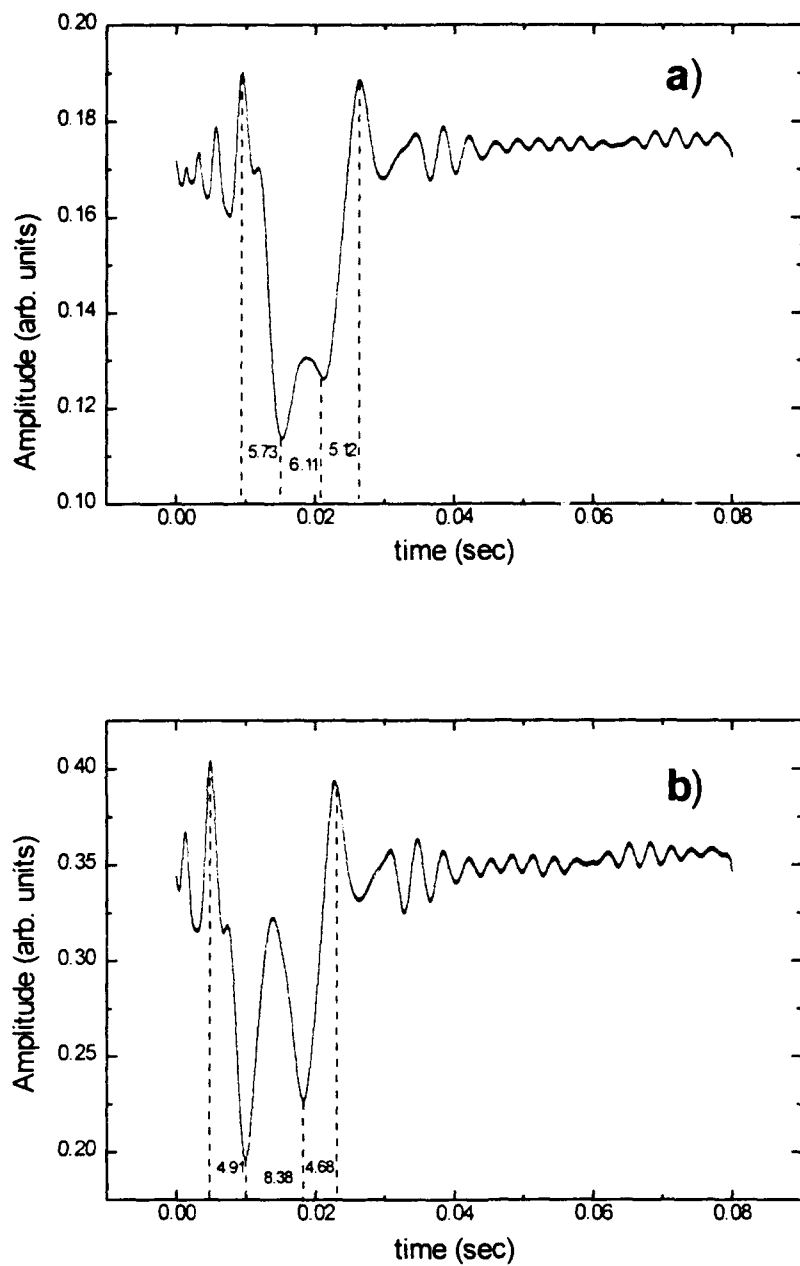


**Fig. 5.7** Modulation envelope of a 4500 Hz carrier wave at 7.69 m the source showing peak to peak time intervals. The intensity level at the source is: a) 144 dB, and b) 156 dB.

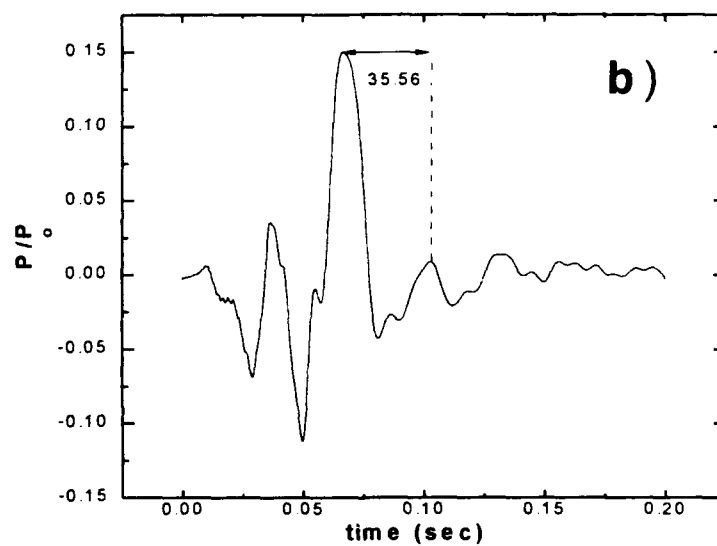
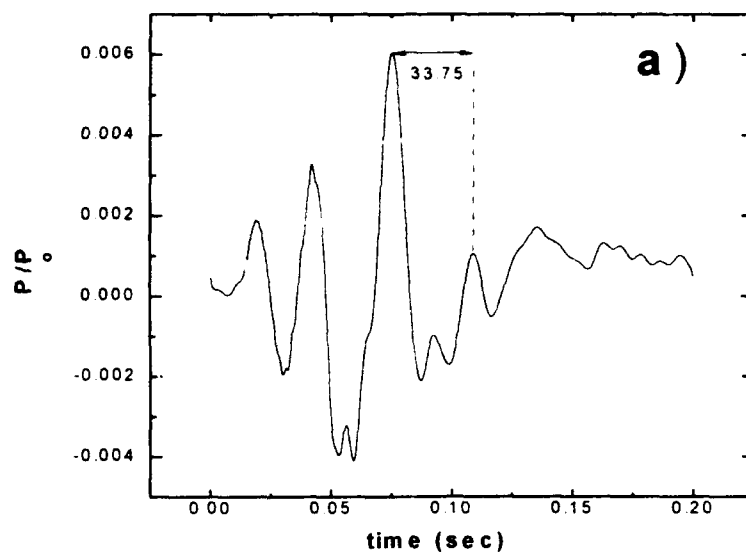


**Fig. 5.8** Envelope a 50 cycle burst at a frequency 4.2 kHz at 10.74 m from the drivers. The acoustic intensity at the source is a) 150 dB and b) 178 dB.

## CHAPTER 6. CONCLUSIONS, POTENTIAL APPLICATIONS, AND FUTURE WORK

### 1. CONCLUSIONS

This work reports the results of theoretical and experimental investigations involving the phenomena of group velocity splitting. We have presented a quantitative derivation of group velocity splitting and given a comprehensive description of the process whereby a modulation of finite extent splits into two separate disturbances traveling with two different velocities of propagation. Also, we have predicted that for modulationally stable nonlinear dispersive systems, a consequence of group velocity splitting is to introduce a frequency modulation component into an amplitude modulated signal.

We have made the first experimental observations of the change in wavelength with amplitude for a mode above cutoff in an cylindrical acoustic duct. The experimental value obtained is within 12% of the theoretical prediction.

To our knowledge, we have made the first experimental observation of pulse splitting in a nonlinear dispersive medium. Experiments show that a single 10 ms duration high amplitude (156 dB ) pulse propagating 7.69 m down the waveguide splits into two pulses traveling at different speeds. Specifically, a single peaked modulated acoustic signal is observed to split into two peaks separated in time by 4.1 ms in fair agreement with theory. Additionally, since the

spreading of the pulse at these distances is not described by dispersion, we conclude that the observed spreading of the modulation at small propagation distances is also a result of group velocity splitting.

## **2. POTENTIAL APPLICATIONS**

The importance of establishing experimentally the effect of group velocity splitting lies in the possible application to fiber optic communication, command, and control links. For example, potential applications could include use of pulse splitting in fiber optic networks requiring increased data redundancy.

The linear group velocity of guided waves in dielectric fibers is determined by a combination of the material dispersion and geometrical waveguide dispersion. In the frequency range of visible light and for a small difference between the clad and the core material, the material dispersion dominates and the dispersion is negative. However if one uses cladding having much smaller index of refraction than the core or longer wavelengths a positive dispersion results because geometrical dispersion dominates in the first case and material dispersion becomes anomalous in the second. Under these conditions pulse splitting becomes possible.

For optical fibers with a positive dispersion, another potential application of the effects presented in this work is the possibility of an all optical AM-FM conversion.

Finally, the effects of group velocity splitting in coastal shallow water acoustics should be studied. For example, potential applications exist in the use of pulse splitting as a littoral environment mine countermeasure.

### **3. FUTURE WORK**

Future work should include continued investigation of the pulse splitting phenomena using input signals of smooth modulation. The splitting appears to be more easily observable for pulses of this type.

Future experiments should also include determination of the relationship between the relative phase and the square of the wave amplitude for a range of frequencies above cutoff. As predicted by the theory presented in Chapter 4, the nonlinear coefficient changes sign for frequencies above 1.897 times the cutoff frequency. For this frequency range, modulational instabilities lead to the formation of solitons. To our knowledge, no experimental observation of acoustic solitons has been made. A future experiment should explore this possibility.

Experimental verification of the predicted AM-FM conversion effect should also be pursued.

## REFERENCES

A.B. Coppins, 1966: " Exact Solutions for the Propagation of Two Simple Acoustic Transients in Waveguides with Perfectly Reflecting Walls," *J. Acoust. Soc. of Am.*, **40** , 331-341

Stephen J. Dorff, 1991: *Apparatus for Measuring the Absorption of Sound by Noise in One Dimension*, Master's Thesis, Naval Postgraduate School, Monterey, California

Joseph B. Keller and Martin H. Millman, 1971: " Finite-Amplitude Sound-Wave Propagation in a Waveguide," *J. Acoust. Soc. of Am.*, **49**, 329-333

L.D. Landau and E.M. Lifshitz, 1959: *Fluid Mechanics* ( Pergmon, Oxford )

Philip M. Morse and K. Uno Ingard, 1968: *Theoretical Acoustics* ( McGraw Hill, New York )

G.B. Whitham, 1974: *Linear and Nonlinear Waves* ( Wiley Interscience, New York )



## INITIAL DISTRIBUTION LIST

- |  |   |
|--|---|
| 1. Defense Technical Information Center<br>Cameron Station<br>Alexandria, Virginia 22304-6145  | 2 |
| 2. Library, Code 52<br>Naval Postgraduate School<br>Monterey, California 93943-5002  | 2 |
| 3. Andrés Larraza<br>Physics Department, Code PH / La<br>Naval Postgraduate School<br>Monterey, California 93943-5002                      | 5 |
| 4. Prof. Anthony A. Atchley<br>Department of Physics, Code PH / Ay<br>Naval Postgraduate School<br>Monterey, California 93943-5002         | 1 |
| 5. Prof. William B. Colson<br>Chairman<br>Physics Department, Code PH / Cw<br>Naval Postgraduate School<br>Monterey, California 93943-5002 | 1 |
| 6. LT William F. Coleman<br>RT 1, Box 115<br>Red Level, Alabama 36474  | 2 |
| 7. Ashok Gopinath<br>Department of Physics<br>Naval Postgraduate School<br>Monterey, California 93943-5002                                 | 1 |